Bound states and asymptotic limits for quantum chromodynamics in two dimensions

R. C. Brower and W. L. Spence
Department of Physics, University of California, Santa Cruz, California 95064

J. H. Weis
Department of Physics, University of Washington, Seattle, Washington 98195
(Received 17 July 1978)

For quantum chromodynamics in two dimensions in the limit of an increasing number of colors ($N_C \to \infty$) with $g^2 N_C/\pi \equiv m^2$ fixed, the meson bound-state problem requires the solution to 't Hooft's integral equation. For low masses, we express the 't Hooft equation as an explicit matrix problem, which enables us to calculate accurate masses m_n^2, ($n = 0,1,\ldots,50$) and wave functions $\phi_n^{a\bar{b}}(x)$ for the quark (a)-antiquark ($\bar{b}$) bound states. In the large-mass (or WKB) limit, the 't Hooft equation is solved analytically. We obtain the spectrum $m_n^2 = \pi^2 m^2 (n + 3/4) + (m_a^2 + m_b^2)\ln n + C(m_a^2) + C(m_b^2) + O(1/n)$, where $C(m_a^2)$ is explicitly calculated. The corresponding WKB wave function, $\phi^{a\bar{b}}{}_n(x) \simeq \sqrt{2}\, \sin[(n+1)\pi x + \delta_n^{a\bar{b}}(x)]$, has a phase shift $\delta_n^{a\bar{b}}(x)$, which is crucial for obtaining the following new asymptotic results for meson bound-state amplitudes: (1) The normalization of the scaling term for $e^+e^- \to X$ and $e^-h \to e^-X$ is demonstrated to agree exactly with the parton model.(2) The inclusive cross section for $e^+e^- \to hX$ is given by the sum over quark fragmentation ($a \to h + b$) functions $D_{h/a}(x_F) = |\Phi_n^{ab}(1/x_F)|^2$, where the complex amplitude $\Phi_n^{a\bar{b}}(x)$ is the analytic continuation of the wave function $\phi_n^{ab}(x)$ to $x > 1$. (3) Regge powers are shown to have the correct phase $A \sim s^{\alpha_{a\bar{b}}(0)} e^{-i\pi\alpha_{ab}(0)}$. These calculations explicitly verify that hard (parton) and soft (dual-Regge) physics can indeed be combined and illustrate the new physics resulting from this unification.

I. INTRODUCTION

Our present understanding of the strong interactions is based on two distinct classes of properties. The first consists of the *soft* properties characteristic of the scattering of bound systems, such as Regge power behavior, strong forward and backward peaks, and very rapidly falling contributions to form factors. The second consists of the *hard* properties associated with pointlike properties and includes Bjorken scaling, the production of jets at all angles in all kinds of reactions with only power-law suppression, and the asymptotic power behavior of form factors. Dual models[1] give a good qualitative description of soft properties while parton models[2] provide an understanding of hard properties.

The present enthusiasm for the confinement hypothesis for the non-Abelian gauge theory of quarks and gluons, quantum chromodynamics (QCD), is based in part on the possibility it offers for a synthesis of the hard and soft properties of strong interactions. In spite of substantial progress, however, such a synthesis is far from having been established. The demonstration of hard, scaling, properties proceeds from QCD using asymptotic freedom, but often relies on a continuation from the deep Euclidean region and ultimately rests upon the perturbation expansion. In fact many hard-scattering properties (e.g. the Drell-Yan formula and all jet lore) do not strictly follow from asymptotic freedom at all. Understanding soft phenomena is even more difficult, though some progress has been achieved by either replacing the bare vacuum by virtual gluonic states[3] or by introducing a compact lattice version[3] of QCD. Since the approximations made in applying QCD in four dimensions are very different for hard and soft phenomena, an important outstanding question about strong interactions is whether QCD or *any single model* can give a synthesis of hard and soft properties. And if such a synthesis can be found, what will be the connecting relationships between, and the boundaries of, each domain?

At present there is only one model which appears to give such a synthesis, namely 't Hooft's $1/N_C$ expansion of QCD in two space-time dimensions[4] (QCD_2). It is important to be very certain that this synthesis is indeed achieved within a *single* approximation scheme.

In the $1/N_C$ expansion [N_C = number of colors, i.e., the gauge group is $SU(N_C)$] the S matrix is written entirely in terms of mesons with only valence quark constituents and their couplings. All scattering amplitudes can be written in a dual loop expansion[1] as overlap integrals involving the wave function for a hadron state $|n,p\rangle$ to consist of a quark a of momentum q and an antiquark $\bar{b}$, which in the $A_- = 0$ gauge is the gauge-invariant null-"plane" matrix element

$$\phi_n^{a\bar b}(x) = \lim_{N_C\to\infty}\left(\frac{N_C}{\pi}\right)^{1/2}\int dy_+ e^{-iy_+(1-2x)p_-} \times \langle 0|\bar\psi_b(-y)\psi_a(y)|n,p\rangle|_{y_-=0} \tag{1.1}$$

as a function of the Lorentz-invariant ratio $x=q_-/p_-$. This wave function is determined by 't Hooft's integral equation.[4] Thus the calculation of hadronic amplitudes essentially reduces to the problem of solving the 't Hooft equation.

Knowledge of three types of properties of this equation is therefore crucial to any demonstration of the consistency of this scheme.

(1) Nature of the spectrum. Confinement requires that it be discrete.

(2) Analytic structure of $\phi_n^{a\bar b}(x)$. Essential for crossing and duality.

(3) Asymptotic (large n) behavior of $\phi_n^{a\bar b}(x)$ and m_n^2. Necessary for the calculation of both hard and soft asymptotic limits, hence for verification of parton properties and Regge behavior.

Discreteness of the spectrum seemed plausible from the beginning and has now been proved.[5] However, the other properties have not been so well studied with the result that until now there have been significant gaps in the derivation of the scaling and analytic properties of the amplitudes. In this paper we will study the 't Hooft equation and extract some salient properties not given in the pioneering work of 't Hooft, Einhorn, and others,[4,6,7] which help to remove these gaps and verify that hard and soft physics are being successfully combined.

It is instructive to note the gaps in particular, together with what was known about hadron scattering amplitudes in QCD_2 when this research was started.

(1) Scaling in annihilation[6,7]:

$$R=\frac{\sigma(e^+e^-\to\text{hadrons})}{\sigma(e^+e^-\to\mu^+\mu^-)} = N_C\sum_a Q_a^2\left(\frac{m_{0a}}{\pi m}\int_0^\infty d\xi\,\frac{\phi^a(\xi)}{\xi}\right)^2.$$

To agree with deep Euclidean asymptotic freedom the coefficient of Q_a^2 should be 1.

(2) Scaling in deep-inelastic electron-hadron scattering[7]: $F(x)\propto[Q_a\phi_n^{a\bar b}(x)]^2+[Q_b\phi_n^{\bar b a}(x)]^2$, but correct normalization was not demonstrated.

(3) Drell-Yan formula for $hh'\to\gamma^*X$ obtained,[8] but normalization again was not shown.

(4) Inclusive annihilation: $\sigma(\gamma^*\to hX)$ scales[9] but parton interpretation was obscure.

(5) "Regge" behavior for meson-meson scattering $A\sim e^{-i\phi}s^{\alpha_{a\bar b}(0)}$ with $\alpha_{a\bar b}(0)=-\beta_a-\beta_{\bar b}$.[10,11] Correct phase $\phi=\pi\alpha_{a\bar b}(0)$ was not shown.

(6) Multi-Regge and Mueller-Regge behavior[12]: Phases were not explicitly calculated.

(7) Form factors $F\sim|q^2|^{-1-\beta}$ with corrections to naive dimensional counting,[7] but with spacelike and timelike limits not demonstrably consistent with analyticity.

(8) Wide-angle (180°) behavior of exclusive amplitudes $A\sim s^{-2-2\beta}$ with similar modification of naive dimensional counting.[11]

(9) Dual Pomeron,[12,13] $A\sim(is/N_C^2)\times$ (zero): Decoupling only because of lack of transverse color charge separation in one space dimension.

Although the list on the whole represents an impressive fusion of parton and Regge lore, the gaps are disturbing because they all point to a lack of understanding of the analytic and asymptotic properties of the scattering amplitudes and leave open the possibility that a major flaw lurks in this area. In previous work[14] we have shown that the formal analytic structure is normal despite the fact that the confining potential introduces a new type of singularity which plays a subtle role in the substructure of the model. Here we develop the mathematical techniques necessary to do explicit asymptotic calculations and fill in most of the gaps in the above list. In a future publication[15] we will discuss physical aspects of the new dual parton model which emerges.

In Sec. II we review the derivation and some general properties of 't Hooft's equation. We then show that the wave function $\phi_n^{a\bar b}(x)$ can be continued into the complex x plane and has only branch points at $x=0,1$. Finally we discuss an approximate method for solving 't Hooft's equation which is well adapted for numerical work and present some typical results.

In Sec. III we study the solutions of 't Hooft's equation for large n. We show that, to $O(1/n)$,

$$m_n^2\simeq\pi^2m^2(n+\tfrac34)+(m_a^2+m_b^2)\ln n + C(m_a^2)+C(m_b^2) \tag{1.2}$$

and

$$\phi_n^{a\bar b}(x)\simeq\sqrt2\sin[(n+1)\pi x+\delta_n^{ab}(x)]\,, \tag{1.3}$$

where

$$\pi\delta_n^{a\bar b}(x) = -m_a^2[(1-x)\ln n+\ln x] - (1-x)[C(m_a^2)-\tfrac18\pi^2m^2] + m_b^2[x\ln n+\ln(1-x)] + x[C(m_b^2)-\tfrac18\pi^2m^2] \tag{1.4}$$

and

$$C(m_a^2)=m_a^2\int_0^\infty dy\left[\frac{1-2y/\sinh 2y}{y\coth y+m_a^2}-\frac{1}{(y^2+2\pi^2)^{1/2}}\right]-m_a^2\,, \qquad (1.5)$$

where m_a^2, m_b^2 are renormalized quark masses and $m^2\equiv g^2N_C/\pi$.

Some of the details of the calculation and an alternate derivation are given in Appendixes A and B. We compare the WKB mass formula (1.3) with the numerical results of Sec. II and find good agreement even for n not too large for typical values of the quark masses.

In Sec. IV we apply the results of Sec. III to study the asymptotic limits of a number of processes in QCD_2. We first recall how the conjectured relationship,[7] for which we give a proof in Sec. III,

$$\int_0^\infty d\xi\frac{\phi^a(\xi)}{\xi}=\frac{\pi}{(1+m_a^2/m^2)^{1/2}}\,, \qquad (1.6)$$

where

$$\phi^a(\xi)\equiv\lim_{n\to\infty}\phi_n^{a\bar{b}}(\xi/\mu_n^2) \qquad (1.7)$$

is necessary for the proof that the deep Euclidean scaling results for annihilation and deep-inelastic scattering can be analytically continued to give correctly the average behavior in the physical region [points (1) and (2) above]. We then study the meson inelastic form factor in the case of one excited meson and explicitly verify that the spacelike and timelike regions are related by analytic continuation using the WKB wave functions (1.4) [point (7) above]. Then we study inclusive annihilation and give the details of the proof[14] that the scaling function is related to the analytic continuation of the deep-inelastic structure function [point (4) above]. Finally we show that the meson-meson scattering amplitude (with one initial and one final meson excited) has the behavior $(-s)^{\alpha_{a\bar{b}}(0)}$ expected on the basis of analyticity [point (5) above]. Some details of this calculation are relegated to Appendix C. All these explicit calculations rely heavily on the WKB wave functions and phase shifts. They can be regarded as explicit checks of the formal proofs of analyticity given in Ref. 14.

II. THE 't HOOFT INTEGRAL EQUATION

A. Formalism

We consider two-dimensional QCD in the $N_C\to\infty$ limit (infinite numbers of colors) with g^2N_C fixed. In this limit the field theory can be reformulated entirely in terms of the scattering of color-singlet meson bound states. The argument, given in detail in the literature,[4] is as follows. Consider the perturbation series for the QCD Lagrangian

$$\begin{aligned}\mathcal{L}&=\tfrac{1}{4}G_{\mu\nu i}{}^{j}G^{\mu\nu i}{}_{j}\\&\quad+\bar{q}^{ai}(i\partial\!\!\!/\delta_i^j+igA\!\!\!/_i{}^j-m_{0a}\delta_i^j)q_j^a\,,\\G_{\mu\nu i}{}^{j}&=\partial_\mu A_{\nu i}{}^{j}-\partial_\nu A_{\mu i}{}^{j}+g[A_\mu,A_\nu]_i{}^j\,,\end{aligned} \qquad (2.1)$$

where $A_i^{\mu j}$ are the traceless $N_C\times N_C$ matrix fields for the gluon $(i,j=1,\ldots,N_C)$ and q_i^a are the quark fields of various colors $(i=1,\ldots,N_C)$ and flavors $(a=1,\ldots,N_f)$. As $N_C\to\infty$ (with g^2N_C fixed) planar diagrams with no quark loops dominate. The crossed diagrams required by Bose and Fermi statistics are order $1/N_C$ because there are very large numbers of distinguishable fields. We then introduce light-cone coordinates

$$x_\pm=x^\mp=\frac{x_0\pm x_1}{\sqrt{2}} \qquad (2.2)$$

and work in the light-cone gauge $A_-=0$. In two dimensions, there are no transverse gluons, all self-coupling of the gluon vanish, and the only gluonic effect is the instantaneous (in x^+) potential[16]

$$D(x)=\frac{i}{2}\,|x^-|\,e^{-\epsilon|x^-|}\delta(x^+) \qquad (2.3)$$

for the longitudinal (A_+) gluon.

Integrals over the gluon potential must be regulated because of strong infrared divergences. A natural regularizaion prescription is just the Fourier transformation of our cutoff potential (2.3),

$$\mathrm{P}\frac{1}{k_-^2}\equiv\frac{1}{2}\left[\frac{1}{(k_-+i\epsilon)^2}+\frac{1}{(k_--i\epsilon)^2}\right], \qquad (2.4)$$

which is referred to as the principal-value prescription.[17] Although this is equivalent to the original chopping procedure of 't Hooft,[4] as emphasized by Einhorn,[7] the principal-value prescription is more convenient. With it all bound-state Green's functions are finite and have only the phases dictated by unitarity in physical regions, but analyticity for crossing quark lines is destroyed. However, we have proved[14] that there are no ill effects for the analyticity of physical color-singlet bound state, or current amplitudes in leading order of $1/N_C$.

We should remark that Wu[18] has recently pointed out that gauge invariance of QCD_2 in the axial gauges (of which the light-cone gauge is a special case) may not hold if the principal-value prescription of Eq. (2.4) is used. He has proposed an alternate regularization procedure which leads to a bound-state equation different from 't Hooft's that is much more difficult to solve. Since the problem of gauge invariance has not yet been fully resolved[19] we shall retain 't Hooft's original formulation of QCD_2 in the light-cone gauge. The evident self-consistency of this formulation and its equivalence to a string model[20] make it physically relevant for the study of the parton-dual Regge synthesis irrespective of the resolutions of this gauge invariance problem.

By writing the perturbation series in the light-front formalism (or old-fashioned $\tau = x^+$ ordered perturbation theory), one notices that to all orders in $g^2 N_C$ (but perburbatively in $1/N_C$) the problem reduces to solving for only one nonperturbative quantity, the quark-antiquark scattering amplitude,

$$iT(q,q',p) = \frac{+ig^2}{(q_- - q'_-)^2} + 4g^2 N_C \times \mathrm{P}\int \frac{d^2k}{(2\pi)^2}\frac{S^a(k)S^{\bar b}(p-k)}{(k_- - q_-)^2}T(k,q,p)\,, \tag{2.5}$$

where

$$S^a(k) = \frac{k_-}{2k_+k_- - m_a{}^2 + i\epsilon} \tag{2.6}$$

is the renormalized quark propagator ($m_a{}^2 \equiv m_{0a}{}^2 - g^2 N_C/\pi$).

From this integral equation follows the homogeneous eigenvalue equation for the bound-state-quark (a)-antiquark ($\bar b$) vertex $\Gamma_n^{a\bar b}(q_-/p_-)$. Finally it is more convenient to introduce the scaling wave function $\phi_n^{ab}(x)$ by

$$\phi_n^{a\bar b}(x) = \frac{\frac{1}{2}\theta(x(1-x))}{p_+ - m_a{}^2/2q_- - m_b{}^2/2(p_- - q_-)}\frac{1}{p_-}\Gamma_n^{a\bar b}(x)\,, \tag{2.7}$$

which satisfies the 't Hooft integral equation

$$m_n{}^2\phi_n^{a\bar b}(x) = \left(\frac{m_a{}^2}{x} + \frac{m_b{}^2}{1-x}\right)\phi_n^{a\bar b}(x) - m^2\mathrm{P}\int_0^1 dy\,\frac{\phi_n^{a\bar b}(y)}{(x-y)^2}\,, \tag{2.8}$$

where we have introduced the Feynman fractional momenta $x = q_-/p_-$ for the quark a and $1-x = (p_- - q_-)/p_-$ for the antiquark $\bar b$. The quantity $m^2 = g^2N_C/\pi$ is the basic mass scale in the theory. In the rest of the paper[21] we use units in which $g^2N_C/\pi = 1$ and the bound mass $m_n{}^2$ is replaced by $\mu_n{}^2 = m_n{}^2/m^2$.

As you might expect, this last equation (2.8) is just the momentum-space Schrödinger equation for the total p_+ in the bound state. In terms of the operators, $H = H_0 + V$,

$$H_0^{a\bar b} = \frac{m_a{}^2}{x} + \frac{m_b{}^2}{1-x}\,, \qquad V = -\mathrm{P}\int_0^1 dy\,\frac{1}{(y-x)^2}\,, \tag{2.9}$$

we note that the total $p_+ = \mu_n{}^2/2p_-$ has quark contributions

$$\frac{m_a{}^2}{2xp_-} + \frac{m_b{}^2}{2(1-x)p_-}$$

in $(1/2p_-)H_0$ and gluon contributions in $(1/2p_-)V$, and

$$\mu_n{}^2\phi_n^{a\bar b}(x) = H\phi_n^{a\bar b}(x)\,. \tag{2.10}$$

Equivalently V may be thought of as a string potential of the Nambu dual string in $d=2$.[20] All the properties of the $1/N_C$ expansion (order by order) follow from the properties of the 't Hooft wave equation.

B. Review of general properties for 't Hooft wave equation

The entire spectrum is discrete[5] ($\mu_n{}^2$, $n = 0,1,2,\ldots$) so the quark-antiquark scattering amplitude can be written

$$T(xp_-, x'p_-, p_-) = \frac{g^2}{(x-x')^2p_-{}^2} - \frac{\pi}{N_C}\frac{1}{p_-{}^2}\sum_{n=0}^{\infty}\frac{\Gamma_n^{a\bar b}(x)\Gamma_n^{a\bar b}(x')}{p^2 - \mu_n{}^2 + i\epsilon}\,. \tag{2.11}$$

The absence of a $q\bar q$ continuum and the related cancellation of the p_+ denominator in $\phi_n^{a\bar b}(x)$ [by a zero in $\Gamma_n^{a\bar b}$, cf. Eq. (2.7)] proves confinement for $d=2$ in leading order in $1/N_C$. The wave functions $\phi_n^{a\bar b}$ are orthogonal and complete,

$$\int_0^1 dx\,\phi_n^{a\bar b}(x)\phi_m^{a\bar b}(x) = \delta_{nm}\,, \qquad \sum_{n=0}^{\infty}\phi_n^{a\bar b}(x)\phi_n^{a\bar b}(x') = \delta(x-x')\,, \tag{2.12}$$

and obey the parity and boundary conditions

$$\phi_n^{a\bar b}(x) + (-)^{n+1}\phi_n^{b\bar a}(1-x) = 0\,, \qquad \phi_n^{a\bar b}(x) \simeq x^{\beta_a}C_n^{a\bar b}\,,\quad x\to 0 \tag{2.13}$$

where β_a is a parameter between 0 and 1 obeying

$$\pi\beta_a\cot\pi\beta_a = -m_a{}^2\,. \tag{2.14}$$

These properties as well as approximate eigenvalues $\mu_n{}^2$ are discussed thoroughly in the literature.[4,6]

In the original paper by 't Hooft,[4] it was pointed out that for large n an approximate wave function is

$$\phi_n^{a\bar b}(x) \simeq \sqrt{2}\sin[(n+1)\pi x]\,, \tag{2.15}$$

and computing $\mu_n{}^2 = \int_0^1\phi_n(x)H\phi_n(x)dx$ one obtains

$$\mu_n{}^2 \simeq n\pi^2 + (m_a{}^2 + m_b{}^2)\ln n + \text{const.} \tag{2.16}$$

However, better large-n (WKB) approximations are actually needed to take scaling and Regge limits for the scattering amplitudes. (See Sec. IV.)

C. Analytic properties of wave function

The wave function $\phi_n^{a\bar{b}}(x)$ as it appears in the Feynman rules [see Eq. (2.7)] is only defined for real x and it vanishes outside $0 \leq x \leq 1$. However, it is straightforward to see that it can be analytically continued into the entire complex plane. We call this extension $\Phi(z)$ so that $\Phi(z=x) \equiv \phi(x)$ for the wave function with $x \in [0,1]$. Suppose that $\phi_n^{a\bar{b}}(x)$ is differentiable[5] so that we can use another definition for the principal-value prescription,

$$P\frac{1}{(x-y)^2} = \frac{1}{(y-x\pm i\epsilon)^2} \pm i\pi\delta'(x-y). \qquad (2.17)$$

The 't Hooft integral equation now takes the form

$$\mu_n^2\phi_n^{a\bar{b}}(x) = H_0^{a\bar{b}}(x)\phi_n^{a\bar{b}}(x) - i\pi\frac{d}{dx}\phi_n^{a\bar{b}}(x) - \int_0^1 dy\frac{\phi_n^{a\bar{b}}(y)}{(y-x+i\epsilon)^2}. \qquad (2.17')$$

Treating the integral as an inhomogeneous term in a first-order differential equation, we may formally solve for $\phi(x)$ (which we call $\Phi(z)$ except when $z = x \in [0,1]$):

$$\Phi_n^{a\bar{b}}(z) = \frac{i}{\pi}\int_{z_0}^{z} dw \exp\left\{\frac{i}{\pi}\int_w^z dx'\left[\mu_n^2 - H_0^{a\bar{b}}\right]\right\} \times \int_0^1 dy\frac{\phi_n^{a\bar{b}}(y)}{(y-w+i\epsilon)^2} + \Phi_n^{a\bar{b}}(z_0). \qquad (2.18)$$

One sees immediately that this defines $\Phi_n^{ab}(z)$ as an analytic function in the cut plane with cuts running to infinity from $z=0$ and $z=1$ along the negative and positive real axes, respectively. The singularities at $z=0,1$ arise from the collision of singularities in the integrand with the end points $y=0,1$ and end points of the integration over w. For $z\approx 0$ $(z\approx 1)$ this gives rise to power-law branch points $\Phi_n^{ab}(z) \sim z^{\beta_a}$ $[\sim(1-z)^{\beta_b}]$. Since $\Phi_n^{ab}(1)=0$, it is often convenient to choose $z_0=1$ in Eq. (2.18). It is easy to show that real analyticity and parity require

$$\Phi_n^{a\bar{b}}(z) = (-)^n\Phi_n^{b\bar{a}}(1-z) = \Phi^{a\bar{b}*}(z^*). \qquad (2.19)$$

Finally, for $z \to x \in [0,1]$ on the first sheet

$$\Phi_n^{a\bar{b}}(x) = \phi_n^{a\bar{b}}(x) \qquad (2.20)$$

because the representation for $\Phi(z)$ in this case is precisely equivalent to the 't Hooft equation (2.17'). This rather trivial observation is the essential ingredient for preserving analyticity of the bound-state scattering amplitudes as shown in Ref. 14.

The analytic function $\Phi(z)$ is *not* to be confused with Einhorn's analytic function (Appendix A of Ref. 7, also employed in Ref. 22) of which $\Phi_n^{a\bar{b}}(x)$ is the imaginary part for $x \in [0,1]$. His function is not the analytic extension of $\phi(x)$ but is rather related essentially to the analytic extension of $\Gamma_n^{a\bar{b}}(x)$ defined originally for $x>1$.

D. Numerical solution of the wave equation

To obtain solutions to the 't Hooft equation one must usually resort to approximation techniques. The only known exception to that is the ground-state solution

$$\phi_0^{ab}(x) = 1, \quad \mu_0^2 = 0 \qquad (2.21)$$

for $m_a^2 = m_b^2 = -1$ (zero bare quark masses). Approximate ground-state eigenvalues are known for small[4] bare quark masses,

$$\mu_0^2 \simeq \frac{\pi}{\sqrt{3}}(m_{0a}+m_{0b}), \qquad (2.22a)$$

and for heavy[23] quarks,

$$\mu_0 \simeq m_{0a}+m_{0b} + (1.019\ldots)\left(\frac{\pi}{2}\right)^{2/3}\left(\frac{m_{0a}+m_{0b}}{2m_{0a}m_{0b}}\right)^{1/3}. \qquad (2.22b)$$

In Sec. III, we give eigenvalues and eigenvectors for $n\to\infty$ up to $O(1/n)$. However, numerical approaches readily give very accurate eigenvalues and eigenfunctions for the low-lying bound states $(n \lesssim 50)$, as verified by comparison with the analytical results above and those to be found in the next section.

We use the series first applied to this problem by Hanson, Peccei, and Prasad[24] to recast 't Hooft's integral equation as a matrix eigenvalue problem which, in truncated form, is amenable to machine solution. The wave functions are representable on the space of C^∞ functions[24] $\sin(m\theta)$ which vanish at the end points on $\theta \in [0,\pi]$ where m is an integer and $x = (1+\cos\theta)/2$,

$$\phi_n^{ab}(x) = \sum_{m=1}^{\infty} a_m \sin[m \arccos(2x-1)]. \qquad (2.23)$$

The integral equation inverts to a matrix equation for the coefficients a_m,

$$(H_0+V)_{ml}a_l = \mu^2 a_m, \qquad (2.24)$$

where H_0 and V have the elements

$$(H_0)_{ml} = \frac{4}{\pi}m_a^2\int_0^\pi d\theta\frac{\sin m\theta \sin l\theta}{1+\cos\theta},$$

$$V_{ml} = -\frac{4}{\pi}\int_0^\pi d\theta \sin m\theta P\int_0^\pi d\theta'\frac{\sin\theta' \sin l\theta'}{(\cos\theta-\cos\theta')^2}.$$

These integrals are evaluated explicitly to get[25]

$$(H_0)_{ml}=[(-)^{l+m}m_a{}^2+m_b{}^2]4\min(l,m)\,,$$

$$V_{ml}=V_{m-1,l-1}+\begin{cases}0\,, & l+m=\text{odd}\\ \dfrac{8l}{(l+m-1)}\,, & l+m=\text{even}\,.\end{cases} \qquad (2.25)$$

The reader may have already noticed the amusing fact that the matrix V is not symmetric (i.e., not Hermitian since it is real). The expansion functions $\sin m\theta$ are orthogonal in the weighted measure

$$\int_0^\pi d\theta=\int_0^1\frac{dx}{[x(1-x)]^{1/2}}$$

while the eigenfunctions are orthogonal in

$$\int_0^1 dx=\int_0^\pi d\theta\frac{\sin\theta}{2}\,.$$

The expansion functions are thus nonunitary transformations effecting a change of basis in which 't Hooft's integral operator becomes an algebraic operator at the price of manifest reality of the spectrum and identity of left and right eigenfunctions. The eigenfunctions are then normalized by dividing by $\sum_l b_l a_l$ where the components of the left eigenfunctions are

$$b_l=\sum_m\int_0^\pi d\theta\frac{\sin\theta}{2}\sin l\theta\sin m\theta\, a_m$$

$$=\sum_{l+m=\text{even}}\left(\frac{2lm}{[(l+m)^2-1][(l-m)^2-1]}\right)a_m\,.$$

It is essentially this trick of allowing different left and right eigenfunctions that lets us reexpress the integral operator as a matrix whose elements can all be calculated in terms of elementary functions. This is exemplified by the expansion in the functions $\sin m\pi x$ employed in Ref. 22, where the projection integrals cannot be evaluated explicitly.

Truncated, 100×100 (or even somewhat larger) matrices can be rapidly diagonalized by computer, yielding eigenvalues accurate to at least five decimal places for $n\lesssim 50$.

We present typical numerical results in the figures. Figure 1 shows the ground-state mass for mesons composed of two quarks of equal bare mass m_0. For large m_0 we see the approach to the nonrelativistic threshold (2.22b), and for small m_0 the pseudo-Goldstone boson mass formula (2.22a) is approximated. Although we get $\mu_0{}^2$ to essentially vanish for $m_0=0$, our technique does not calculate the ground-state energy very well for very small m_0, giving a result a little too low for $m_0=0.16$ and progressively worsening for m_0 less than that. This is due to the fact that the truncated series (2.23) does not correctly represent the singular end-point behavior of the wave function. Our expansion functions $\sim x^{1/2}\,[\sim(1-x)^{1/2}]$ as $x\to0$ $(x\to1)$ and $\mu_0{}^2$ depends analytically on $m_0{}^2$. The correct ground-state mass estimate derives from[4]

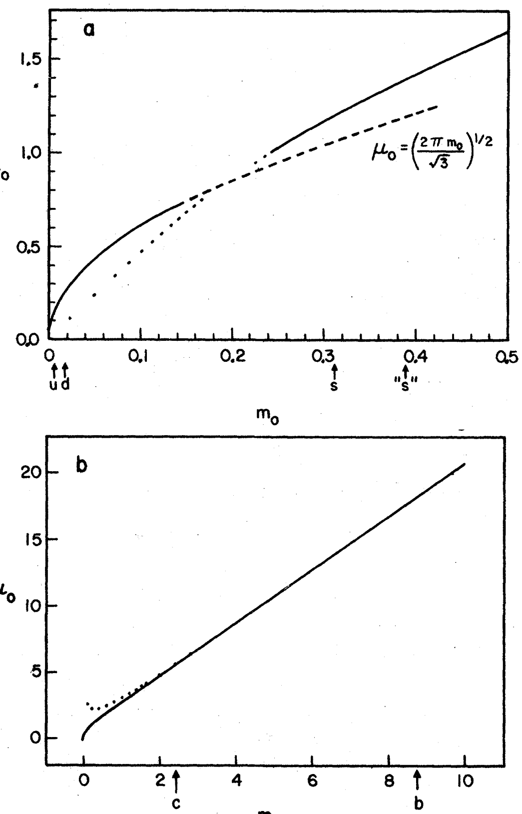

FIG. 1. Ground-state mass μ_0 for mesons composed of quarks of equal bare mass m_0. (a) Small quark masses. We plot the approximation (2.22a) $\mu_0{}^2\simeq(\pi/\sqrt{3})2m_0$ and show in dashes where it breaks down. The unlabeled curve was obtained with our numerical method, shown in dots where it breaks down. It is easy to see how the two solid curves should be joined to give a curve accurate in the whole domain. By setting $g^2N_C/\pi^2\alpha_0'\approx(581\text{ MeV})^2$ we set the unit of mass equal to 581 MeV and make the identifications shown for the physical quark masses, corresponding to $m_{0u}\approx6.2$, $m_{0d}\approx11.1$, and $m_{0s}\approx195$, all in MeV. "s" denotes the incorrect value of the strange-quark mass which would be obtained with the approximate formula which is seen to be invalid in the region. (b) Large quark masses, computed numerically (solid line), along with the nonrelativistic threshold state formula [dotted line Eq. (2.22b)]. We indicate the charm quark at 1.4 GeV and the b quark at 5.1 GeV.

$$\mu_0{}^2\simeq(m_{0a}+m_{0b})m_{0a}\int_0^1 dx\frac{\phi_0^{ab}(x)}{x}$$

$$\simeq(m_{0a}+m_{0b})\frac{\pi}{\sqrt{3}}\,,$$

where the singular end-point behavior enters crucially. Hence any variational method which uses the exact end-point singularity as input (such as 't Hooft's[4]) should do much better in this particular case.

By choosing $g^2N_C/\pi = (581\text{ MeV})^2$ [to correspond to a Regge slope $\alpha_0' = (3/\pi^2)(g^2N_C/\pi)^{-1} = 0.9/\text{GeV}^2$ according to the construction of Ref. 11], we calculate the masses of the light quarks from the physical pseudoscalar masses using additivity[26] for the u and the d and fitting the strange-quark mass to that of the K^0. For $u\bar{u}$ and $d\bar{d}$ the small quark mass approximation is well satisfied and the u and d masses are small enough for the K masses to be additive, but the dependence on the strange-quark mass is not linear (for the squares of the K masses). We find $m_{0s} \approx 195$ MeV and $m_{0s}/m_{0d} \approx 18$ (rather than 224 MeV and 20 as the approximation would imply[26]). The mass squared of the $s\bar{s}$ bound state is then not precisely additive and we find $m_{s\bar{s}} \approx 740$ MeV rather than 687 MeV. This implies $m_8 \approx 610$ MeV and suggests that η-η' mixing is somewhat larger than usually supposed. The differences between the model and reality are sufficiently great that we do not take these numbers seriously, but regard these results as an amusing indication of what may in fact happen.

Although the Lagrangian of the theory is defined only for $m_a^2 \geq -1$, i.e., real m_{0a}, 't Hooft's equation appears to be defined for all m_a^2, and the numerical method can be applied for $m_a^2 < -1$. Interestingly enough, we find that the ground state immediately becomes tachyonic as m_a^2 is lowered through -1, and that more and more tachyons (starting with the ground state and extending up to some definite n) appear in the spectrum as m_a^2 becomes more negative.

We will show our numerical results for excited

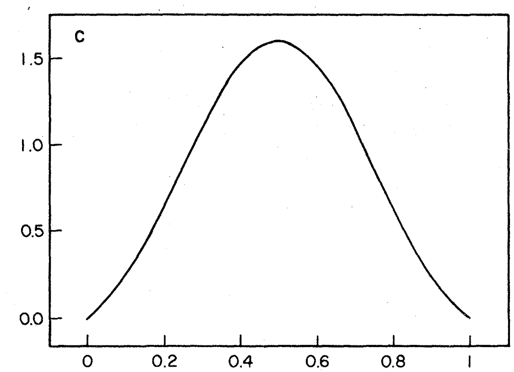

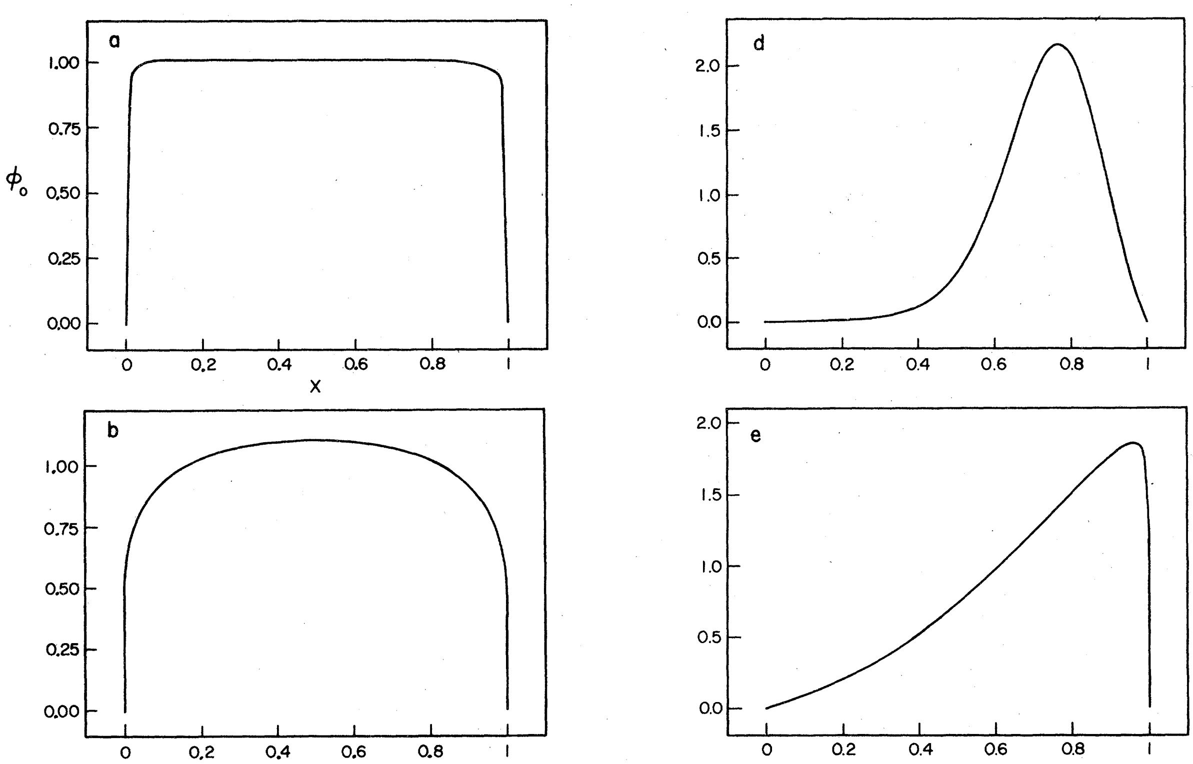

FIG. 2. Ground-state wave functions $\phi_0^{\bar{a}b}(x)$ for various combinations of physical quarks, as obtained numerically. (a) $a=b=$down (b) $a=b=$strange (c) $a=b=$charm (d) $a=b$-quark, $b=$charm (e) $a=$charm, $b=$down. In drawing the figures we have smoothed out the small high-frequency oscillations which are inevitable in truncated Fourier series expansion methods.

states in the next section where we compare them with the WKB approximation developed there.

We also find that the numerical method can easily be used to compute eigenfunctions. In Fig. 2 we present typical ground-state wave functions for various combinations of the physical quark masses just determined. In Fig. 3 we show examples of the $n=4$ excited state. Here we also plot the WKB formula (derived in the limit $n\to\infty$) to be obtained in Sec. III. We see that the numerical method and the WKB approximation, except for the case of the b quark (which has very large $m_b^2 \simeq 76m^2$), effectively corroborate each other. It is especially striking that this happens for small values of n. In fact we find that the location of the single node in the first excited state wave function is accurately given by the WKB formula (3.1a) for reasonably small values of the quark masses. In the next section we give an illustration showing that the numerical method also gives accurate results (confirmed by the WKB result) for $n\approx 50$.

This numerical technique differs from those

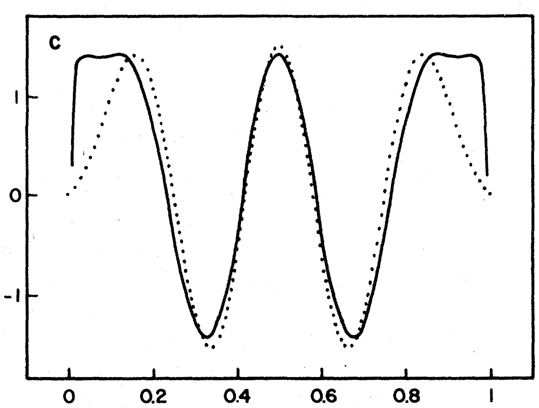

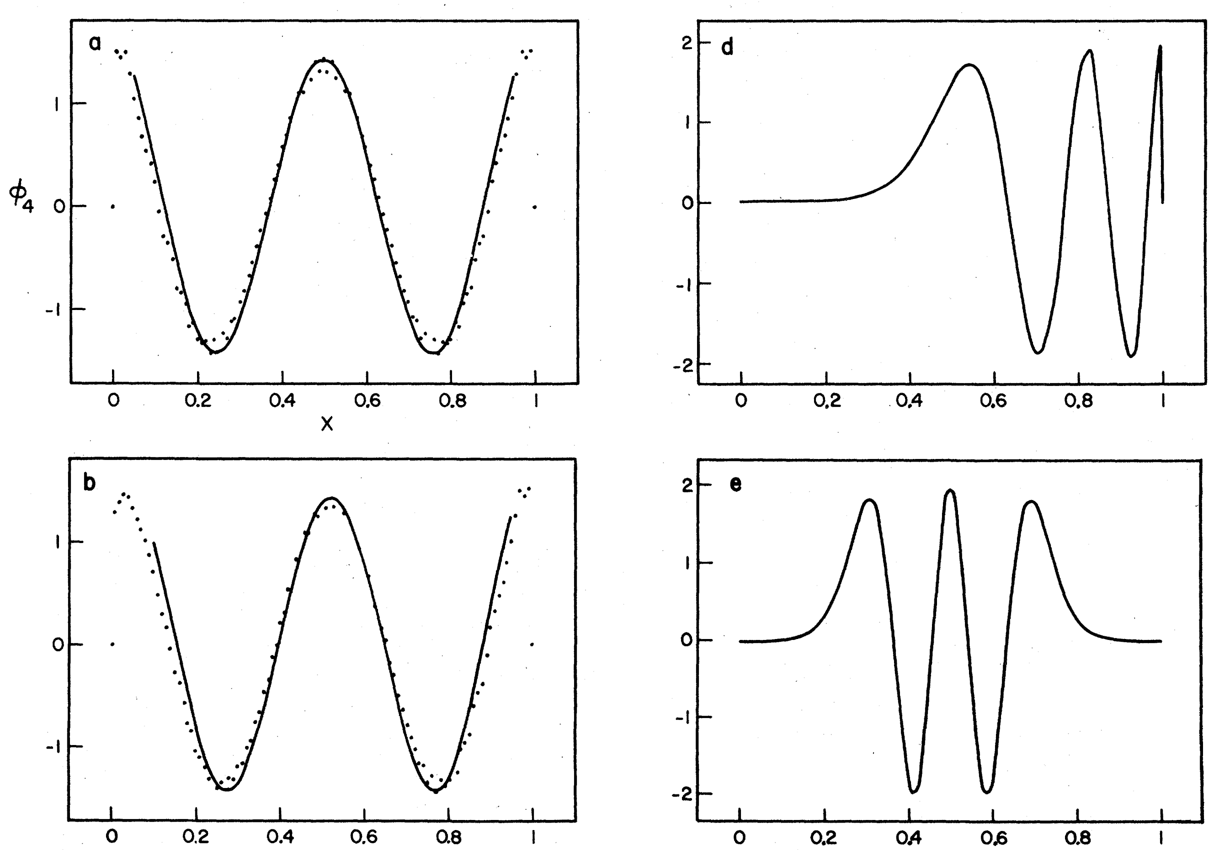

FIG. 3. Excited state ($n=4$) wave functions $\phi_4^{\bar{q}b}(x)$. The WKB formula derived in Sec. III is shown as a solid line together with points obtained by the numerical method for various combinations of the physical quark masses. (a) $a=b$ = down (b) a = strange, b = down (c) $a=b$ = charm (d) $a=b$-quark, b = down (e) $a=b=b$-quark. In (d) and (e) we plot only the numerical results (as a solid line) since the WKB formula fails for such a low n state of such a heavy quark.

previously applied to this equation. 't Hooft and collaborators[4] used a variational method on trial wave functions which treats the power-law branch point at the end points of $\phi(x)$ exactly, but is limited by the fact that variational calculations become prohibitive as the number of parameters gets large. We are able to employ our method for larger eigenvalues, corroborate our extended WKB approximation ('t Hooft was unable to verify the coefficients of the $\ln n$ pieces in the eigenvalue), and show that the validity of the WKB approximation extends to rather small n. Hanson *et al.*[24] use the same expansion [Eq. (2.23)] but follow closely the Multhop method of aerodynamicists and construct a finite dimensional matrix by evaluating the uninverted equation at a particular set of angles. They note that their method seems to fail badly for the lowest eigenvalue in the case in which the bare quark masses approach zero where the exact answer is rigorously known to be zero (the decoupled Goldstone boson). We find $\mu_0^2 \cong 0$ to within the limits of computational accuracy. We hope that techniques similar to ours will prove useful in analyzing the bound-state spectrum of the radial relativistic wave equations that arise in (string) approximations to the four-dimensional field theory.

III. THE WKB APPROXIMATION FOR 't HOOFT INTEGRAL EQUATION

A. Semiclassical argument

It is desirable to know the full WKB solution to the 't Hooft equation. Namely for large n, we seek wave functions and masses

$$\phi_n^{a\bar{b}}(x) \simeq \sqrt{2}\sin[(n+1)\pi x + \delta_n^{a\bar{b}}(x)] , \tag{3.1a}$$

$$\mu_n^2 \simeq \pi^2 n + (m_a^2 + m_b^2)\ln n + C(m_a^2, m_b^2) \tag{3.1b}$$

up to order $1/n$ terms where the phase shift $\delta_n^{a\bar{b}}$ and the constant C must be determined analytically. Since the rigorous derivation from the integral equation is quite involved, it is enlightening to first recast the problem in a semiclassical form to see the general idea. On a classical level the coordinate conjugate to $x = q_-/p_-$ is the separation between the quarks $p = x_a^- - x_b^-$ (we call this "p" since it is conjugate to Bjorken's x). Hence for $H_{\text{classical}} = [H_0(x) + V(p)]/\pi$,

$$H_{\text{classical}} = \frac{1}{\pi}\left(\frac{m^2}{x} + \frac{m_b^2}{1-x}\right) + |p| . \tag{3.2}$$

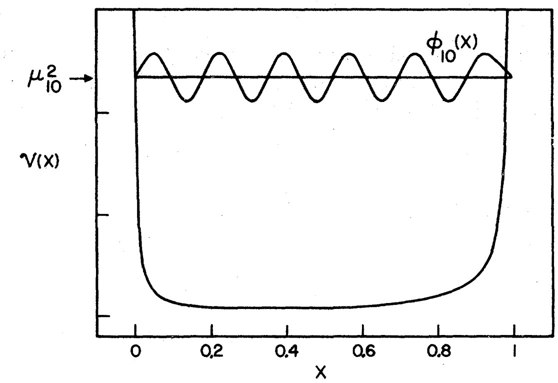

FIG. 4. "Photon" in the "Coulomb" potential $\pi\mathcal{V}(x) = 1/2x + 2/(1-x)$.

Remarkably by switching the role of kinetic and potential energy (as we have switched the notation for x, p coordinates) this is recognized as a "photon" ($E_{\text{kinetic}} = |p|$) in a "Coulomb" potential

$$\mathcal{V}(x) = \frac{1}{\pi}\left(\frac{m_a^2}{x} + \frac{m_b^2}{1-x}\right) = \frac{1}{\pi} H_0^{a\bar{b}}(x) . \tag{3.3}$$

The standard WKB procedure for this problem is to use the classical orbits $\dot{p} = (\partial/\partial x)\mathcal{V}$, $\dot{x} = \pm 1$, and calculate the classical action

$$S_n^{a\bar{b}}(x) = \int^x dx' p = \int^x [E_n - \mathcal{V}(x')]dx' \tag{3.4}$$

for energy $E_n = \mu_n^2/\pi$. We will demonstrate that this indeed leads to the WKB wave function

$$\phi_n^{a\bar{b}}(x) \simeq \sqrt{2}\,\mathrm{Im}\, e^{-iS_n^{a\bar{b}}(x)} . \tag{3.5}$$

However, as usual the tricky problem is to compute the phase shift of the reflected wave near the classical turning point, so that the integration constant in (3.4) can be fixed by the eigenvalue conditions for a closed orbit

$$\oint p\, dx = 2\pi\left(n + \frac{1}{\pi^2} C(m_a^2, m_b^2)\right) . \tag{3.6}$$

For the 't Hooft equation this is particularly delicate, since the classical turning point is separated by only order $1/n$ from the singularities in the potential (see Fig. 4). Only a precise quantum treatment of the boundary regions ($0 \leq x \leq 1/n$, $0 < 1 - x < 1/n$) will suffice.[27]

B. Interior WKB solution

We now proceed to the derivation of the WKB formula. Consider the trial wave function $\sqrt{2}\sin[(n+1)\pi x + \delta_n^{a\bar{b}}(x)]$ in 't Hooft's equation (2.8), and using (2.17) distort the contour (in the complex $y=y_R+iy_I$ plane) up (down) for the $e^{i[(n+1)\pi y+\delta(y)]}$ $(e^{-i[(n+1)\pi y+\delta(y)]})$ piece of the integrand (see Fig. 5). The result is easily seen to be

$$[\mu_n^2-\pi^2(n+1)-H_0^{a\bar{b}}(x)-\pi\delta'(x)]\sqrt{2}\sin[(n+1)\pi x+\delta_n^{a\bar{b}}(x)]=\sqrt{2}\int_0^\infty dy_I\left\{e^{-(n+1)\pi y_I}\,\mathrm{Re}\left[\frac{e^{i\delta_n^{a\bar{b}}(iy_I)}}{(x-iy_I)^2}-(iy_I\to iy_I+1)\right]\right\}. \tag{3.7}$$

Thus for the interior region $\epsilon \le x \le 1-\epsilon$ with any small ϵ, the right-hand side is of order $1/n$ and we have the differential equation for $\delta_n^{a\bar{b}}(x)$,

$$\mu_n^2-\pi^2(n+1)-H_0^{a\bar{b}}(x)=\pi\frac{d}{dx}\delta_n^{a\bar{b}}(x)\,, \tag{3.8}$$

which determines $\delta_n^{a\bar{b}}(x)$ up to a constant. To fix this constant we must look closely at the boundary layer regions $x\sim O(1/n)$ and $1-x\sim O(1/n)$.

By rescaling $x=\xi/\mu_n^2\simeq\xi/\pi^2 n$ at fixed ξ one can introduce the boundary layer function[28]

$$\phi^a(\xi)=\lim_{n\to\infty}\phi_n^{a\bar{b}}(\xi/\mu_n^2)\,, \tag{3.9}$$

which is easily shown to satisfy a limiting form (as $n\to\infty$) of 't Hooft's equation[7]

$$\phi^a(\xi)=\frac{m_a^2}{\xi}\phi^a(\xi)-\mathrm{P}\int_0^\infty d\eta\frac{\phi^a(\eta)}{(\eta-\xi)^2}. \tag{3.10}$$

Now we may determine the unknown WKB constants by *demanding* a matching condition in the boundary layer. Namely the interior (WKB) solution must scale as

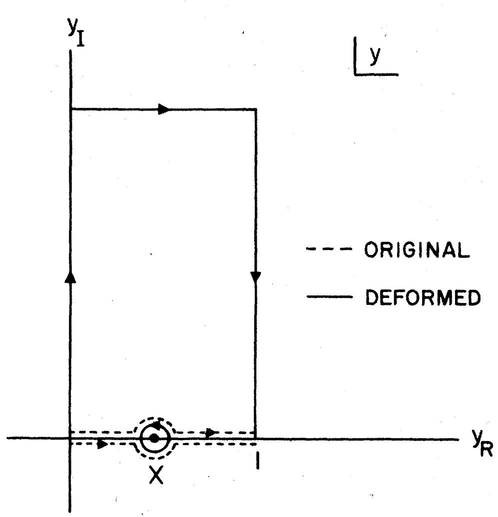

FIG. 5. Contour distortions used in deriving the interior WKB solution.

$$\sqrt{2}\sin[(n+1)\pi x+\delta_n^{a\bar{b}}(x)]\simeq\sqrt{2}\sin[\xi/\pi+\delta^a(\xi)] \tag{3.11}$$

for $n\to\infty$ at fixed $\xi>0$ (i.e., $x\simeq\xi/\pi^2 n$) and conversely that the boundary layer function must go over to the WKB form

$$\phi^a(\xi)\simeq\sqrt{2}\sin[\xi/\pi+\delta^a(\xi)] \tag{3.12}$$

as $\xi\to\infty$. Although this boundary condition appears hard to implement, it already restricts the dependence of the integration constants on m_a^2 and m_b^2 because $\phi^a(\xi)$ [or $\phi^b(\xi)$] is independent of the opposite boundary's mass m_b^2 (or m_a^2).

Substituting

$$\mu_n^2\simeq\pi^2 n+(m_a^2+m_b^2)\ln n+C(m_a^2,m_b^2) \tag{3.13}$$

into our differential equation, we have

$$\begin{aligned}\pi\delta_n^{ab}(x)=&-m_a^2[(1-x)\ln n+\ln x]\\&+m_b^2[x\ln n+\ln(1-x)]\\&+(x-\tfrac{1}{2})[C(m_a^2,m_b^2)-\pi^2]+C_0(m_a^2,m_b^2)\,,\end{aligned} \tag{3.14}$$

where we have used the symmetry condition

$$\phi_n^{a\bar{b}}(x)+(-)^{n+1}\phi_n^{b\bar{a}}(1-x)=0\,. \tag{3.15}$$

We now impose the condition (3.12) that $\delta^{a\bar{b}}(\xi/n\pi^2)\to\delta^a(\xi)$ independent of $\bar{b}$ as $n\to\infty$. It is straightforward to see that this requires $C(m_a^2,m_b^2)$ and $C_0(m_a^2,m_b^2)$ to be given in terms of one unknown function $C(m_a^2)$ so that $C(m_a^2,m_b^2)=C(m_a^2)+C(m_b^2)+3\pi^2/4$, where in our definition of $C(m^2)$ we have *anticipated* the result $C(0,0)=3\pi^2/4$ given below. Hence we have the solution

$$\begin{aligned}\pi\delta_n^{a\bar{b}}(x)=&-m_a^2[(1-x)\ln n+\ln x]-(1-x)\left[C(m_a^2)-\frac{\pi^2}{8}\right]\\&+m_b^2[x\ln n+\ln(1-x)]+x\left[C(m_b^2)-\frac{\pi^2}{8}\right]\end{aligned} \tag{3.16a}$$

and

$$\pi\delta^a(\xi) = -m_a^2 \ln(\xi/\pi^2) - C(m_a^2) + \frac{\pi^2}{8}, \qquad (3.16b)$$

where the same constants also enter into the mass spectrum

$$\mu_n^2 \simeq \pi^2(n+\tfrac{3}{4}) + (m_a^2 + m_b^2)\ln n + C(m_a^2) + C(m_b^2). \qquad (3.17)$$

To compute $C(m_a^2)$ in principle we need only to find the boundary layer function $\phi^a(\xi)$ and take the limit $\xi\to\infty$.

C. Boundary layer function

The reduction of the WKB problem to computing the boundary function $\phi(\xi)$ appears at first sight to have just replaced 't Hooft's equation (2.8) with an equally troublesome integral equation (3.10). However, the boundary layer equation (3.10) convolutes the unknown function with the kernel over a semi-infinite interval so we may replace it by a difference equation in a transformed representation.[29] That is, from

$$\phi^a(\xi) = \frac{m_a^2}{\xi} - \mathrm{P}\int_0^\infty d\eta \frac{\phi^a(\xi)}{(\eta-\xi)^2} \qquad (3.18)$$

we obtain the difference equation

$$\psi(\lambda+1) = (\pi\lambda\cot\pi\lambda + \beta\pi\cot\pi\beta)\psi(\lambda) \qquad (3.19)$$

for the transformed function

$$\psi(\lambda) = \int_0^\infty d\xi\, \xi^{\lambda-1}\phi^a(\xi). \qquad (3.20)$$

The λ plane is a kind of quark J plane since λ is conjugate to the quark rapidity. Since any solution to the difference equation can have an arbitrary multiplicative periodic function $[P(\lambda) = P(\lambda+1)]$, we must also add supplementary conditions. From the definition of $\psi(\lambda)$ and the behavior of $\phi^a(\xi)$ for small ξ,

$$\phi^a(\xi) \sim \xi^\beta, \qquad (3.21)$$

and for large ξ [Eq. (3.12)], we see that $\psi(\lambda_R + i\lambda_I)$ is analytic for $-\beta<\lambda_R<1$. Moreover, we can calculate the dominant term for $\lambda_I\to\pm\infty$ from the WKB portion of the integral (Λ arbitrarily large)

$$\psi(\lambda_R+i\lambda_I) \simeq \int_\Lambda^\infty d\xi\, \xi^{\lambda_R-1}\xi^{i\lambda_I}\sqrt{2} \times \sin[\xi/\pi + \delta(\xi)]. \qquad (3.22)$$

Using (3.16b) and stationary phase to evaluate the integral as $\lambda_I\to\infty$ we have (see Appendix A)

$$\psi(\lambda_R+i\lambda_I) \simeq \pi(\pi\lambda_I)^{\lambda_R+i\lambda_I-1/2}\exp\left\{\frac{i}{\pi}\left[C(m_a^2)+\frac{\pi^2}{8}+m_a^2\ln\left(\frac{\lambda_I}{\pi}\right)-\pi\lambda_I\right]\right\}. \qquad (3.23)$$

Analyticity in the strip $(-\beta<\lambda_R<1)$, real analyticity $\psi(\lambda^*)=\psi(\lambda)$, and this asymptotic condition for $|\psi(\lambda)|$ *uniquely* fixes the solution to the difference equation. We proceed to give the solution to the difference equation for $m_a^2=0$ $(\beta=\frac{1}{2})$ and refer the reader to Appendix B for the general solution as an infinite product. There $C(m_a^2)$ is computed by direct computation of $\psi(\lambda_R+i\lambda_I)$ and its $\lambda_I\to\infty$ limit. Here we resort to an indirect argument for $m_a^2\neq 0$.

For $m_a^2=0$, the difference equation is

$$\psi_0(\lambda+1) = \pi\lambda\tan\pi\lambda\,\psi_0(\lambda). \qquad (3.24)$$

Avoiding the temptation to write down a trivial solution such as $\psi_0(\lambda)=\Gamma(\lambda)(\tan\pi\lambda)^\lambda$, which has a disastrous essential singularity at $\lambda=1/2$, we look at the logarithmic derivative

$$\frac{d}{d\lambda}\ln\psi_0(\lambda+1) = \frac{1}{\lambda} + \frac{2\pi}{\sin 2\pi\lambda} + \frac{d}{d\lambda}\ln\psi_0(\lambda). \qquad (3.25)$$

From this the solution with no singularities for $-\beta\leq \mathrm{Re}\lambda\leq 1$,

$$\psi_0(\lambda) = \psi_0(1)\pi^{\lambda-1}\Gamma(\lambda) \times \exp\left[-2\pi\int_0^{\lambda-1} du\frac{u+\frac{1}{2}\sin^2\pi u}{\sin(2\pi u)}\right], \qquad (3.26)$$

is not too difficult to ascertain (see Appendix B). The real normalization constant $\psi_0(1)$ is not yet known. Then using Sterling's formula we can compute its asymptotic behavior:

$$\psi_0(\lambda_R+i\lambda_I) \simeq \psi_0(1)(\pi\lambda_I)^{\lambda_R+i\lambda_I-1/2} \times e^{i(\pi/8-\lambda_I)}. \qquad (3.27)$$

Comparison with (3.23) shows that the normalization constant is $\psi_0(1)=\pi$ and from the phase we find

$$C(0)=0. \qquad (3.28)$$

This verifies 't Hooft's conjecture for $m_a^2=m_b^2=0$ that

$$m_n^2 \simeq \left(\frac{g^2N_C}{\pi}\right)\pi^2(n+\tfrac{3}{4}) + O\left(\frac{1}{n}\right). \qquad (3.29)$$

Curiously, we find $n+\frac{3}{4}$ instead of the $n+\frac{1}{2}$ which is usual in nonrelativistic quantum mechanics. (However, $\frac{1}{4}$ integer shifts do occur in the WKB approximation for the radial equation with $1/r$ centrifugal terms.) In general the shift in relativistic problems depends on the details.[30]

We can now compute $C(m_a^2)$ for general m_a^2 by the following trick, which actually avoids explicitly constructing the solution $\psi(\lambda)$ to the difference equation. Consider the contour integral (see Fig. 6)

$$\oint_{\mathcal{C}} d\lambda' \ln\psi(\lambda') = i\int_{-\lambda_I}^{\lambda_I} d\lambda_I \ln\left[\frac{\psi(\lambda_R+i\lambda_I+1)}{\psi(\lambda_R+i\lambda_I)}\right] + \int_{\lambda_R}^{\lambda_R+1} d\lambda_R' \ln\left[\frac{\psi(\lambda_R+i\lambda_I)}{\psi(\lambda_R-i\lambda_I)}\right] = 0\,. \tag{3.30}$$

The integral is zero because the meromorphic solution $\psi(\lambda)$ we seek has no poles and no zeros inside the contour, as we now argue.

For any meromorphic function with analytic dependence on a parameter m_a^2 a zero can disappear only if, by variation of m_a^2, it can be made to coincide with a pole. Conversely, a zero can be created under infinitesimal variation only if a pole is also created infinitesimally close by; the zero-pole pair then separates if the variation is increased. By our boundary conditions $\psi(\lambda)$ has no poles in D, the infinite strip $-\beta \le \lambda_R \le 2$ containing $\mathcal{C}$. For $m_a^2=0$ the explicit solution $\psi_0(\lambda)$ has no zeros in D. By the analytic dependence on m_a^2 at $m_a^2=0$ of the difference equation there will therefore still be no zeros in D for $|m_a^2|>0$ unless they enter D from the outside, which none can do at least for some finite range in m_a^2 (again by analyticity in m_a^2).

Now we evaluate the contour integral. The two sides bounded by $\lambda_R'=\lambda_R$ and $\lambda_R'=\lambda_R+1$ can be integrated using the difference equation, and for $\lambda_I\to\infty$ the sides at $\lambda_I'=\pm\lambda_I$ are given by the WKB asymptotic condition. Setting the sum equal to zero leads to a formula for $C(m_a^2)$:

$$C(m_a^2)=m_a^2\int_0^\infty dy\left[\frac{(1-2y/\sinh 2y)}{y\coth y+m_a^2}-\frac{1}{y^2+2\pi^2}\right]-m_a^2\,. \tag{3.31}$$

For $m_a^2\to 0$,

$$C(m_a^2)\simeq m_a^2(\gamma+2\ln 2+\ln\pi)\,, \tag{3.32}$$

where γ is Euler's constant, and for $m_a^2\to\infty$,

$$C(m_a^2)\simeq -m_a^2[\ln(m_a^2/\pi^2)-1]\,. \tag{3.33}$$

In Fig. 7 we plot $C(m_a^2)$ for $m_a^2\ge -1(m_{0a}^2\ge 0)$. We obtain the same result by a completely independent method in Appendix B where we find the form of $\psi(\lambda)$ by direct construction. Thus the full WKB problem has an explicit analytic solution.

The result of the direct calculation of $\psi(\lambda)$ in Appendix B can be expressed as an infinite product multiplied by the $m_a^2=0$ solution $\psi_0(\lambda)$:

$$\psi(\lambda)=(1+m_a^2)^{1/2}\psi_0(\lambda)\prod_{n=0}^{\infty}\frac{1+(m_a^2/\pi)\tan\pi\lambda/(\beta_n+n)}{1+(m_a^2/\pi)\tan\pi\lambda/(\lambda+n)}\,, \tag{3.34}$$

where β_n are the roots $(0\le\beta_n\le 1)$ of

$$\pi(\beta_n+n)\cot\pi\beta_n+m_a^2=0$$

so that $\beta_0=\beta$ and $\beta_n\to\frac{1}{2}$ for all n as $m^2\to 0$. This infinite product can be computed in the limit $\lambda_I\to\pm\infty$ [Eq. (B20)] so that the formula for $C(m_a^2)$ is verified and the normalization

$$\psi(0)=\int_0^\infty d\xi\,\frac{\phi^a(\xi)}{\xi}=\frac{\pi}{(1+m_a^2)^{1/2}} \tag{3.35}$$

is fixed. This latter sum rule is the missing link in computing the scaling limit for $e^+e^-\to X$, $eh\to eX$, and the Drell-Yan process $hh'\to e^+e^-X$.

We have found that the region of validity of our numerical solution ($n\lesssim 50$) considerably overlaps the WKB region for reasonable values of the quark masses $m_a^2\lesssim 20$ and that comparison of results gotten from the two methods is illuminating. In Fig. 8 we plot the fractional difference $(\mu_{\rm WKB}^2-\mu_n^2)/\mu_{\rm WKB}^2$, where $\mu_{\rm WKB}^2$ is the formula in Eq. (3.1a) with the replacement $\ln n\to\ln(n+K)$ where K is adjusted in each case to make $\mu_{\rm WKB}^2=\mu_0^2$.

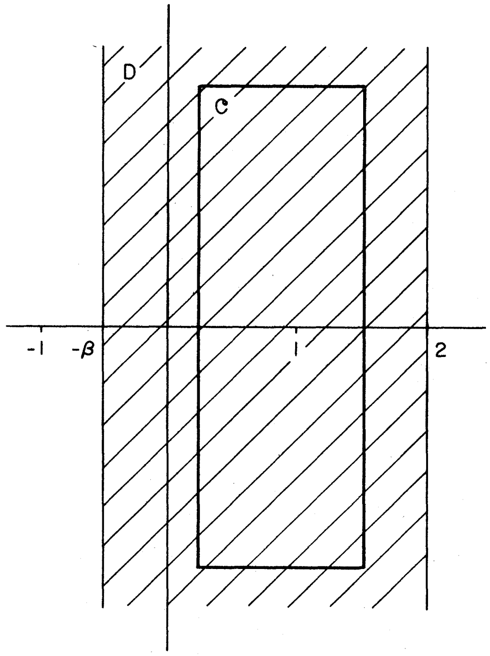

FIG. 6. Contour $\mathcal{C}$ for integral and domain D in which integrand has neither poles nor zeros.

This choice defines the WKB formula for finite n and is practical since it is usually easy to compute the ground state, although it makes a rather arbitrary assignment of $1/n$ corrections. The approach to the WKB limit is surprisingly rapid: For the physical values of the quark masses shown, it is never worse than 20%. The rate at which the WKB limit is approached is dependent

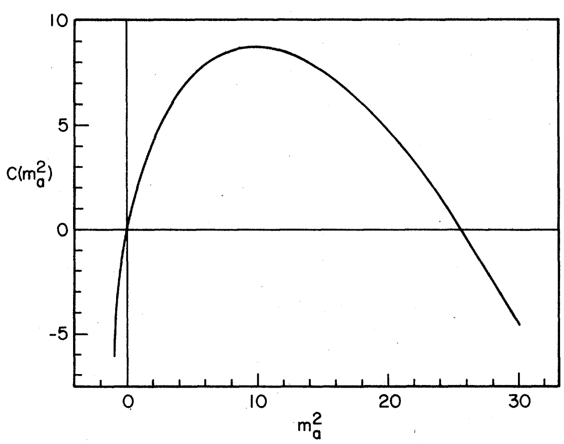

FIG. 7. The WKB constant $C(m_a{}^2)$ computed from Eq. (3.32) for $m_a{}^2 > -1$. The numerical phase shift yields values for $C(m_a{}^2)$ for $m_a{}^2 \leq 10$ which lie exactly on the curve.

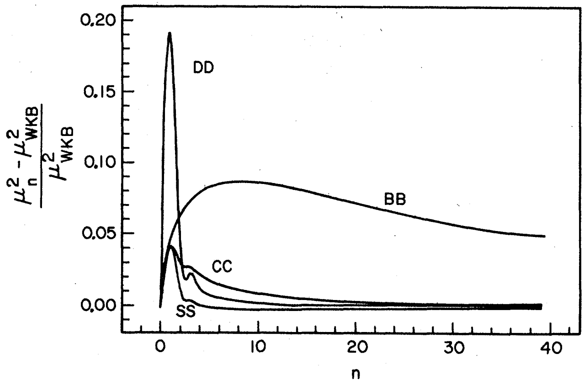

FIG. 8. Comparison of the numerical eigenvalues with the WKB ($n \to \infty$) formula. We plot the fractional difference $(\mu_n{}^2 - \mu_{\text{WKB}}{}^2)/\mu_{\text{WKB}}{}^2$ for $n \leq 40$ for quarkonium with bare quark masses $m_{od} = 11.1$ MeV, $m_{os} = 195$ MeV, $m_{oc} = 1.4$ GeV, $m_{ob} = 5.1$ GeV. Convergence is rapid except for the b quark.

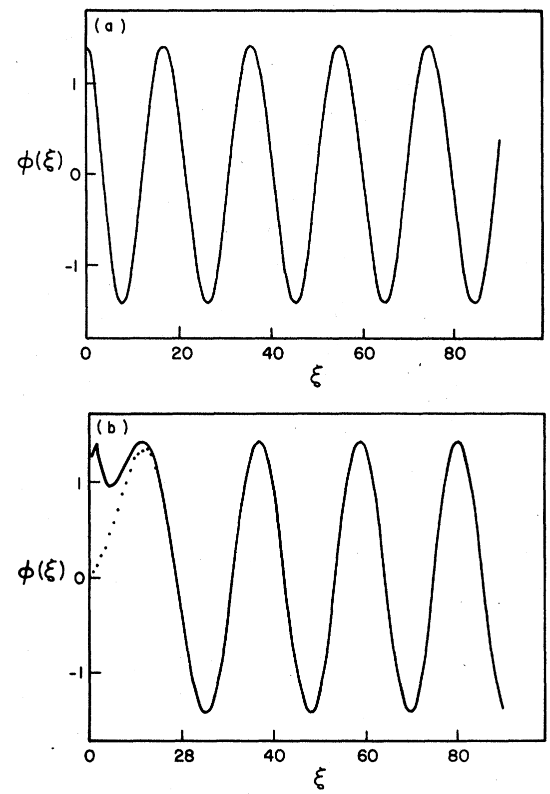

FIG. 9. Boundary layer function $\phi^a(\xi)$ in the WKB approximation (3.12) for $1 \leq \xi \leq 90$ is shown as a solid line. (a) a = down. We expect $\lim_{n\to\infty} \phi_n^{a\bar{b}}(\xi/\mu_n{}^2) = \phi^a(\xi)$ and indeed find that points obtained numerically for $\phi_{50}^{a\bar{b}}(\xi/\mu_{50}{}^2)$ lie on this curve for various $\bar{b}$. (b) a = charm. Here we show $\phi_{50}^{a\bar{b}}(\xi/\mu_{50}{}^2)$, obtained numerically, for b = down in dots which merge with the solid curve before the first node.

on the quark masses, but it is always better than 3% by $n=3$ for the light quarks. For small n and very massive quarks one should of course use the nonrelativistic limit of 't Hooft's equation. However, even for the b quark the interpolation between $\mu_0^2 \approx 4m_0^2$ and μ_∞^2 given by $\mu_{n\,\mathrm{WKB}}^2$ is better than 10%.

The WKB solution is also as accurate for the eigenfunctions. We show examples of the numerical calculation of $\phi_{50}^{ab}(\xi/\mu_{50}^2)$ plotted against the WKB (3.12) calculation of $\phi^a(\xi)$ in Fig. 9.

IV. THE WKB LIMIT AND ASYMPTOTIC AMPLITUDES

A. Hard processes

In the previous two sections we have derived the WKB approximation for eigenvalues and wave functions. As an immediate application of the complete solution for the boundary layer function we proved Eq. (3.35). This demonstrates that the normalization of the deep-inelastic electroproduction and annihilation total cross sections, computed in the physical region, agrees with continuation of the asymptotic freedom result obtained in the deep Euclidean domain, and that the normalization of the cross section for the Drell-Yan process accords with the naive parton prescription.

The physics of why this relation is crucial is essentially the same in all situations, so we illustrate it only for the hallowed case of deep-inelastic lepton-hadron scattering. (We essentially repeat Einhorn's calculation of Ref. 7, to which the reader is referred for more detail.)

Since the intermediate state for $N_C \gg 1$ is exclusively composed of single, nondegenerate, mesons of mass μ_l^2 we need only compute the *amplitude* for $h(n)+\gamma^* \to h(l)$ with $\mu_l^2 = s$. We consider the scaling limit in which $x_B \equiv q_-/p_- \simeq (1-s/q^2)^{-1}$ is fixed as $q^2 \to -\infty$, where q_μ and p_μ are the current and target momenta. The structure function is then proportional to the absolute square of the infinite-momentum frame amplitude of Fig. 10, for which the expression is[31]

$$\frac{1}{\sqrt{\pi}}F \simeq \frac{1}{\sqrt{\pi}}\frac{2}{x_B}(2\sqrt{\pi})^2 \int_{x_B}^{1}\frac{dx}{4\pi}\phi_n^{a\bar b}(x)\phi_l^{a\bar b}\left(\frac{x-x_B}{1-x_B}\right)\bigg|_{l\to s/\pi^2}. \tag{4.1}$$

(There are additional, vector-meson dominance type graphs, but these are negligible in the scaling limit.) In writing the limit we have already used the leading WKB behavior of the eigenvalue $\mu_l^2 \sim l\pi^2$, and we obviously need the WKB eigenfunction to take the limit on $\phi_l^{a\bar b}$. The latter oscillates rapidly, causing (4.1) to vanish, except

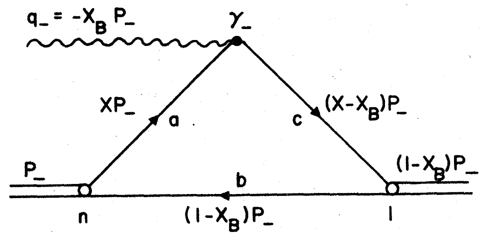

FIG. 10. Infinite-momentum frame diagram for deep-inelastic electroproduction. We label the external lines by the minus light-cone component of their momentum and the vertices by their excitation number. Internal (quark) lines are labeled by their flavor and the minus component of their momentum.

for the contribution of the boundary layer $(x-x_B/(1-x_B) \sim \xi/\mu_l^2$. Thus ϕ_l^{ab} acts like a δ function putting the struck quark near the mass shell,

$$x_{\text{on shell}} \simeq x_B + \frac{x_B m_{0a}^2}{(-q^2)},$$

as if it were being freely produced. Hence we have

$$\frac{1}{\sqrt{\pi}}F \simeq \frac{2}{x_B}2\sqrt{\pi}\phi_n^{a\bar b}(x_B)\left[\frac{1}{2\pi}\frac{x_B}{(-q^2)}\int_0^\infty d\xi\,\phi^a(\xi)\right], \tag{4.2}$$

but we still need to show that the parton-model normalization is obtained, i.e., that the coefficient of the wave function in brackets is just the square root of the two-quark phase space (including the quark "spin" sum):

$$\left[\int\frac{dx}{4\pi}\,\frac{\pi}{2}\,\delta\left(\frac{\mu_n^2}{2}+\frac{q^2}{-2x_B}-\frac{m_{0a}^2}{2(x-x_B)}-\frac{m_b^2}{2(1-x)}\right)\right]^{1/2}$$

$$\simeq \frac{1}{2\pi}\frac{x_B}{(-q^2)}m_{0a}^2\left(\frac{\pi}{m_{0a}}\right). \tag{4.3}$$

This is done by integrating Eq. (3.10) for the boundary layer function to get

$$\int_0^\infty d\xi\,\phi^a(\xi) = m_{0a}^2\int_0^\infty d\xi\,\frac{\phi^a(\xi)}{\xi} = m_{0a}^2\left(\frac{\pi}{m_{0a}}\right), \tag{4.4}$$

where we use our result (3.35) in the last step. Thus we have shown the relevance of our WKB solution in fulfilling parton-model expectations.

B. Soft processes

We now direct our attention to certain soft processes where the interest is even greater since here the application of naive parton ideas is very uncertain. We have found that the full content of our improved WKB formulas is essential for the calculation of many asymptotic amplitudes in situations where more than one mass gets large. We illustrate this effect in the following calculations which we also feel do much to exemplify the union of hard and soft physics being achieved.

(1) We start with a study of the meson transition form factor for $|q^2| \to \infty$ in the case where one meson is very excited[32] (though remaining much less massive than $|q^2|^{1/2}$). By taking $q^2 \to +\infty$ *and* $q^2 \to -\infty$ we show the analytic behavior $(-q^2)^{-\beta_b-1}$, thus giving an explicit example of the analyticity shown formally in Ref. 14 and confirming that the real axis limit (where an infinite number of poles are "smeared" with a $+i\epsilon$ prescription) is being taken correctly.

(2) Next we study the meson form factor in the scaling limit in which $|q^2| \to \infty$ is in fixed proportion to one of the meson masses. We show in detail the calculation[33] of inclusive annihilation ($q^2 \to +\infty$) and how analytic continuation connects it to deep-inelastic ($q^2 \to -\infty$) scattering (part A of this section) via the extension of 't Hooft's wave function developed in Sec. IIC.

(3) Finally we calculate the Regge limit $|s| \to \infty$, $t = 0$ for the quasielastic scattering of a low-mass meson off an excited meson[32] (though of mass $\ll |s|^{1/2}$). We find behavior $\sim(-s)^{-\beta_a-\beta_b}$, again consistent with normal analyticity, thus completing the calculations and verifying the conjectures in Ref. 11.

(i) Asymptotic form factors. For $q^2 \to +\infty$ the amplitude, an exclusive two-body contribution to hadron production in annihilation, is given by the two graphs in Fig. 11:

$$F = 2(2\sqrt{\pi})^4 \sum_l \int_0^1 \frac{dx'}{4\pi} \phi_l^{c\bar a}(x') \frac{1}{q^2 - \mu_l^2 \pm i\epsilon} \left[\int_{x_F}^1 \frac{dx}{4\pi} \phi_l^{c\bar a}(1-x) \frac{1}{x_F} \Gamma_n^{a\bar b}\left(\frac{x}{x_F}\right) \phi_m^{c\bar b}\left(\frac{1-x}{1-x_F}\right) - \int_0^{x_F} \frac{dx}{4\pi} \phi_l^{c\bar a}(1-x) \phi_n^{a\bar b}\left(\frac{x}{x_F}\right) \frac{1}{1-x_F} \Gamma_m^{c\bar b}\left(\frac{1-x}{1-x_F}\right)\right], \tag{4.5}$$

where

$$x_F = \frac{q^2 + \mu_n^2 - \mu_m^2 + (\lambda(q^2, \mu_n^2, \mu_m^2))^{1/2}}{2q^2},$$

and for $x \geq 1$,

$$\Gamma_n^{a\bar b}(x) = \int_0^1 dy \frac{\phi_n^{a\bar b}(y)}{(x-y)^2} \tag{4.6}$$

includes the explicit gluon exchanges and acts like an effective quark $\to$ meson + quark vertex.

For $q^2 \to \infty$ with μ_n^2 and μ_m^2 fixed, $x_F \simeq 1 - \mu_m^2/q^2$ and we can take $\sum_l \simeq (q^2/\pi^2)\int_0^\infty d\lambda$ with $\lambda = l\pi^2/q^2$. We apply (4.4) to get

$$\int_0^1 dx' \phi_l^{c\bar a}(x') \simeq \frac{m_{0c}\pi}{\lambda q^2}. \tag{4.7}$$

The remaining factor receives its dominant contribution from $x \simeq 1 - \xi/q^2$ since $l \simeq \lambda q^2/\pi^2$ and our WKB formula applies to $\phi_l^{ca}(1-x)$, allowing the replacement

$$\phi_l^{c\bar a}(1-x) \simeq \phi^c(\xi).$$

Noting that

$$\frac{1}{x_F}\Gamma_n^{a\bar b}\left(\frac{x}{x_F}\right) \simeq [(\mu_m^2 - \xi)/q^2]^{\beta_b - 1} \frac{\pi\beta_b C_n^{ba}}{\sin\pi\beta_b}$$

for $x/x_F \simeq 1 - (\xi - \mu_m^2)/q^2$, and, furthermore, that

$$\phi_n^{a\bar b}\left(\frac{x}{x_F}\right)\frac{1}{1-x_F} \simeq [(\xi - \mu_m^2)/q^2]^{\beta_b}(\mu_m^2/q^2)^{-1} C_n^{ba},$$

we obtain

$$F \simeq \frac{2m_{0c}}{\pi} C_n^{ba}(q^2)^{-1-\beta_b} \int_0^\infty \frac{d\lambda}{\lambda}(1 - \lambda \pm i\epsilon)^{-1} \left[\int_0^{\mu_m^2} d\xi\, \phi^c(\lambda\xi)(\mu_m^2 - \xi)^{\beta_b - 1} \phi_m^{c\bar b}(\xi/\mu_m^2) \frac{\pi\beta_b}{\sin\pi\beta_b} - \int_{\mu_m^2}^\infty d\xi\, \phi^c(\lambda\xi)(\xi - \mu_m^2)^{\beta_b} \frac{1}{\mu_m^2}\Gamma_m^{c\bar b}(\xi/\mu_m^2)\right]. \tag{4.8}$$

The whole expression can be evaluated if the further limit $\mu_m^2 \to \infty$ is now taken. The second term is then very small since although $(1/\mu_m^2)\Gamma_m^{c\bar{b}} \simeq \int_0^\infty d\eta\phi^b(\eta)/(\eta-\xi)^2$, $\phi^c(\xi)$ oscillates as the range of integration tends to vanish. However, the first term is dominated by the (integrable) singularity at $\xi=\mu_m^2 \to \infty$ so that the interior WKB formulas can be used for both ϕ^c [see (3.12)] and $\phi_m^{c\bar{b}}(\xi/\mu_m^2)$ [see (3.1a)]. Since ξ is not $\ll \mu_m^2$, we cannot use the boundary layer form of $\phi_m^{c\bar{b}}(\xi/\mu_m^2)$ which applies when $\xi/\mu_m^2 \approx O(1/\mu_m^2)$. The other boundary region of this wave function has a width given by $1-\xi/\mu_m^2 \approx O(1/\mu_m^2)$ and is therefore negligible even though the singularity in the integrand occurs at $\xi/\mu_m^2=1$.

It is useful to pause briefly and write the WKB formulas in a slightly different form more suited to this sort of calculation. Since

$$\mu_n^2 \simeq \pi^2(n+\tfrac{3}{4}) + (m_a^2+m_b^2)\ln n + C(m_a^2) + C(m_b^2),$$

the argument in the WKB wave function $\sqrt{2}\sin[(n+1)\pi x + \delta_n^{a\bar{b}}(x)]$ can be rewritten using the explicit formula (3.16a) for $\delta_n^{a\bar{b}}(x)$ and the fact that $\ln n$ and $\ln\mu_n^2/\pi^2$ differ by $O(\ln n/n)$ as

$$\frac{1}{\pi}\left[\mu_n^2 x - m_a^2\ln(\mu_n^2 x/\pi^2) + m_b^2\ln(1-x) - C(m_a^2) + \frac{\pi^2}{8}\right] \equiv \frac{\mu_n^2 x}{\pi} + \zeta_n^{a\bar{b}}(x), \tag{4.9}$$

so we can regard $\zeta_n^{a\bar{b}}(x)$ as the phase shift in the alternate representation explicitly depending only on μ_n^2:

$$\phi_n^{a\bar{b}}(x) \simeq \sqrt{2}\sin[\mu_n^2 x/\pi + \zeta_n^{a\bar{b}}(x)]. \tag{4.10}$$

Note that $\lim_{x\to\xi/\mu_n^2} \zeta_n^{a\bar{b}}(x) = \delta^a(\xi)$.

Returning to the calculation we set

$$\phi^c(\lambda\xi)\phi_m^{c\bar{b}}(\xi/\mu_m^2) \simeq \cos\left[\frac{(\lambda-1)\xi}{\pi} + \delta^a(\xi) - \zeta_m^{c\bar{b}}(\xi/\mu_m^2)\right] + \cos\left[\frac{(\lambda+1)\xi}{\pi} + \delta^a(\xi) + \zeta_m^{c\bar{b}}(\xi/\mu_m^2)\right].$$

Seeing that $\lambda \approx 1$ dominates, the second term oscillates away relative to the first so we drop it and plug in the explicit form for the phase-shift difference

$$\pi[\delta^c(\xi) - \zeta_m^{c\bar{b}}(\xi/\mu_m^2)] = m_b^2\ln(1-\xi/\mu_m^2) - m_c^2\ln\lambda,$$

from which all dependence on quark c cancels for $\lambda=1$ due to the additive nature of the phase shift.

We have now

$$F \simeq 2m_{0c}\frac{\beta_b}{\sin\pi\beta_b} C_n^{ba}(q^2)^{-1-\beta_b}\int_0^\infty \frac{d\lambda}{\lambda}(1-\lambda \pm i\epsilon)^{-1} \times \int_0^{\mu_m^2} d\xi(\xi-\mu_m^2)^{\beta_b-1}\cos\left\{\frac{1}{\pi}[(\lambda-1)\xi - m_c^2\ln\lambda + m_b^2\ln(1-\xi/\mu_m^2)]\right\}.$$

With negligible effect the λ contour can be extended to $-\infty$ and then closed in the half plane appropriate to each exponential piece of the cosine. Note that the more primitive WKB form (2.15) [i.e., without inclusion of the phase shift $\delta_n^{a\bar{b}}(x)$] would essentially miss the cosine factor, give a pure imaginary amplitude, and be inconsistent with analyticity. It seems that the WKB phase shift contributes to asymptotic limits only when two wave functions oscillate rapidly with the same frequency ($\xi/\pi^2 \simeq \mu_m^2/\pi^2$ here) to compensate the vanishing either would cause alone. The overlap integral then becomes very sensitive to any phase difference between the two and knowledge of the phase shift is essential.

The rest of the evaluation is straightforward, using $\pi\beta_b\cot\pi\beta_b = -m_b^2$, we finally get the simple result

$$F \simeq 2\pi C_n^{ba} m_{0c}(q^2 e^{\mp i\pi})^{-1-\beta_b}(\mu_m^2)^{\beta_b}. \tag{4.11}$$

For $q^2 \to -\infty$ and μ_m^2 fixed, we have in addition to the point coupling graph of Fig. 10 the vector dominance type graphs of Fig. 12. Einhorn[7] has shown that in general all three graphs contribute and have the behavior $(-q^2)^{-1-\beta_b}$. But for the special case of $\mu_m^2 \to \infty$, the vector dominance contributions cancel and we have only Fig. 10 which is just (4.2) evaluated for $x_B \sim 1 + \mu_m^2/q^2$,

$$F \simeq 2\pi C_n^{ba} m_{0c}(-q^2)^{-\beta_b-1}(\mu_m^2)^{\beta_b} \tag{4.12}$$

[using the end-point behavior of the wave function (2.13)] for $-q^2 \gg \mu_m^2 \gg 1$. Thus the transition form factor behaves exactly as expected of a cut-plane analytic function of q^2.

These calculations provide an interesting check

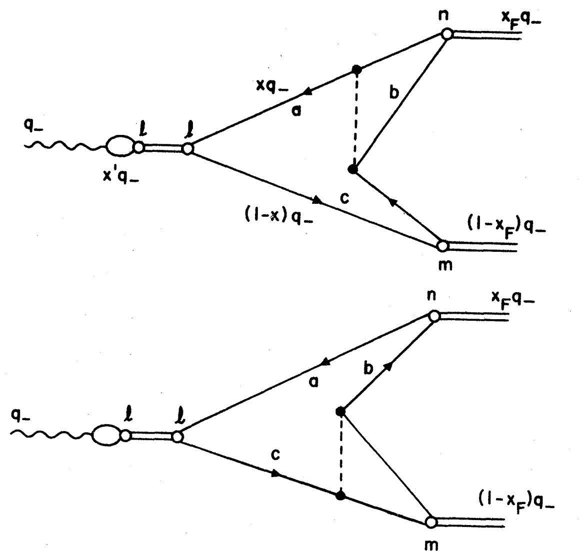

FIG. 11. Diagrams for the production of two mesons by a massive timelike photon. (A dashed line denotes the gluon potential.)

of the more formal analyticity proofs of Ref. 14 and illustrate how the WKB wave functions of Sec. II enter in a crucial way.

(ii) Scaling limit of inclusive annihilation. We now repeat the previous study but allow the mass $\mu_m{}^2$ to increase in fixed ratio with q^2 as $|q^2|\to\infty$. Starting with the case $q^2\to+\infty$, we consider again the diagrams of Fig. 11 and Eq. (4.5). Now $x_F \simeq 1-\mu_m{}^2/q^2$ is fixed, so that $|F|^2$ is in fact proportional to the inclusive annihilation cross section and x_F is the conventional Feynman scaling variable. Exactly as before, $\sum_l \simeq (q^2/\pi^2)\int_0^\infty d\lambda$ with $\lambda=\mu_l{}^2/q^2$ and (4.4) is used, but now we need to take the combined limit $\mu_l{}^2=\lambda q^2\to\infty$ and $\mu_m{}^2=(1-x_F)(q^2-\mu_n{}^2/x_F)\to\infty$ on the three-meson vertex. The oscillations in $\phi_l^{c\bar a}(1-x)$ cause the second term to vanish since the oscillations in $\Gamma_m^{c\bar b}(1-x)/(1-x_F)$ can compensate them only in an infinitesimal region. However, the wave function $\phi_m^{c\bar b}$ in the first term also oscillates, in fact having essentially the same frequency

$$\frac{1-x}{1-x_F}\,\frac{\mu_m{}^2}{\pi^2}\simeq(1-x)\frac{q^2}{\pi^2}.$$

Hence we expect a scaling contribution from the interior WKB region (the boundary layer is of infinitesimal thickness) and invoke again (4.10). Dropping as before a term which oscillates with frequency $O(q^2)$ for $\lambda\approx1$ we make the approximation

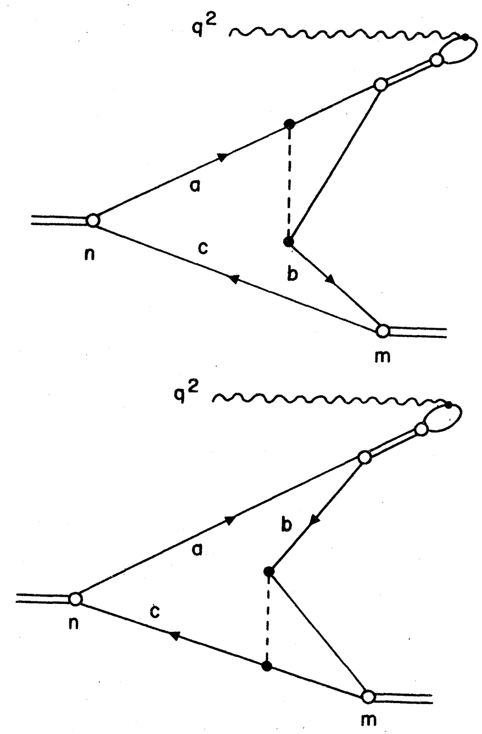

FIG. 12. Vector-meson dominance type contributions to the form factor for $q^2\to-\infty$, which cancel when $\mu_m{}^2\to\infty$.

$$\phi_l^{c\bar a}(1-x)\phi_m^{c\bar b}\left(\frac{1-x}{1-x_F}\right)\simeq\cos\left\{\frac{1}{\pi}\left[(\lambda-1)q^2+\frac{\mu_n{}^2}{x_F}\right](1-x)+\zeta_l^{c\bar a}(1-x)-\zeta_m^{c\bar b}\left(\frac{1-x}{1-x_F}\right)\right\},$$

where the difference in phase shifts tends to

$$\pi\zeta_l^{c\bar a}(1-x)-\pi\zeta_m^{c\bar b}\left(\frac{1-x}{1-x_F}\right)\simeq m_a{}^2\ln x+m_b{}^2\ln\left(\frac{1-x_F}{x-x_F}\right)-m_c{}^2\ln\lambda$$

from which all dependence on quark c cancels when $\lambda=1$. Thus we have

$$F \simeq \frac{m_{0c}}{\pi}\frac{1}{q^2}\frac{1}{x_F}\int_0^\infty \frac{d\lambda}{\lambda}(1-\lambda \pm i\epsilon)^{-1}$$
$$\times \int_{x_F}^1 dx\, \Gamma_n^{a\bar{b}}(x/x_F)\left(\exp\left\{\frac{i}{\pi}\left[(\lambda-1)q^2(1-x) - m_c^2\ln\lambda + \frac{1-x}{x_F}\mu_n^2 + m_a^2\ln x + m_b^2\ln\left(\frac{1-x_F}{x-x_F}\right)\right]\right\} + \text{cc}\right).$$

As in the previous calculation the λ contour can be expanded to $-\infty$ and closed in the appropriate half plane. Making the change of variables $x = x_F w$ to rescale the a quark momentum, giving it now as a fraction w of the momentum of the outgoing state of mass μ_n^2, we write the final result

$$F \simeq 2\pi m_{0c}(1/q^2)\left(\frac{\pm i}{\pi}\int_1^{1/x_F} dw \exp\left\{\frac{\pm i}{\pi}\left[\left(\frac{1}{x_F} - w\right)\mu_n^2 + m_a^2\ln(x_F w) + m_b^2\ln\left(\frac{1/x_F - 1}{w-1}\right)\right]\right\}\Gamma_n^{a\bar{b}}(w)\right) \tag{4.13}$$

for $\mu_m^2 \simeq (1-x_F)^{-1}q^2 \to \infty \pm i\epsilon$. The expression in large outer parentheses is immediately recognizable as the analytic continuation of 't Hooft's wave function, i.e., by (2.18),

$$F \simeq 2\pi m_{0c}(1/q^2)\Phi_n^{a\bar{b}}(1/x_F). \tag{4.14}$$

The argument $1/x_F$ appears since $x_F = 1/x_B$. Therefore this calculation shows that the inclusive annihilation amplitude (4.14) for $0 < x_F < 1$ is the analytic continuation of the deep-inelastic amplitude (4.2) from $0 < x_B < 1$ to $x_B = 1/x_F > 1$.

We note again the importance of our WKB formulas in establishing this result. The exponential factor under the integral in (4.13) arises entirely from the phase difference between the two wave functions and gives the amplitude a nontrivial x_F-dependent phase. There is no reason to believe that such a phase will not also occur in QCD_4—thus it should have phenomenological consequences unanticipated in naive parton models. The quark additivity evidenced in the WKB eigenvalue and phase shift lead to the somewhat remarkable result that the expression in large outer parentheses in (4.13) is independent of quark c, showing that inclusive production can to some extent be thought of as the fragmentation of quark a. Nevertheless it must be emphasized that quarks a and b do not propagate freely but reasonate with quark c and are far from their mass shells.

In Fig. 13 we plot the effective fragmentation function $D_{n/a} = |\Phi_n^{a\bar{b}}(1/x_F)|^2$ for $a \to h(n) + b$ along with the phase angle characterizing the inclusive amplitude

$$\Phi_n^{a\bar{b}}(1/x_F) = e^{i\theta_n^{a\bar{b}}(x_F)}|\Phi_n^{a\bar{b}}(1/x_F)|.$$

The fragmentation function appears to approach a constant as $x_F \to 0$. This would be quite extraordinary since we have only included the diagram in which a single quark-antiquark pair is created—no central plateau is expected in this order of $1/N_C$.[34] However, the plot of the phase angle informs us that the real and imaginary parts of the amplitude actually oscillate rapidly around zero for small x_F. Hence we regard the apparent plateau as an artifact of the precise zero-width nature of the resonances in finite orders in $1/N_C$. It is akin to phenomena already encountered in the dual reso-

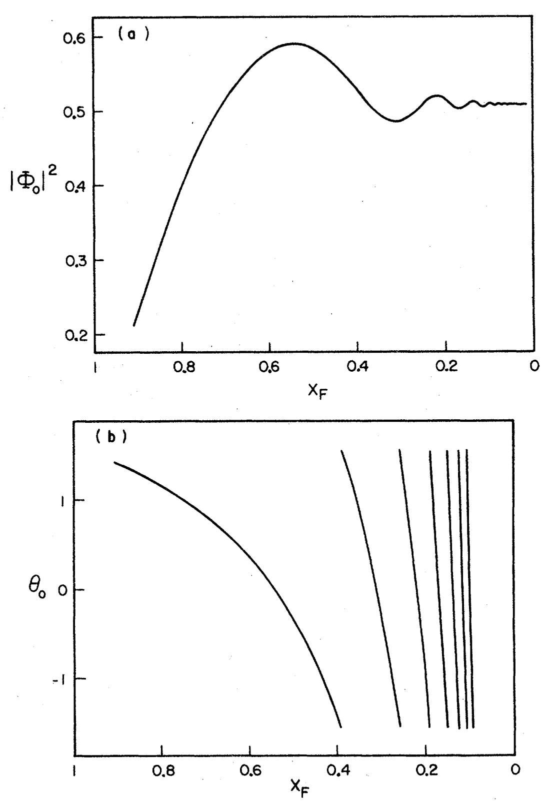

FIG. 13. (a) D function defined in the text for $m_a^2 = m_b^2 = 0$. (b) Phase angle of the inclusive annihilation amplitude.

nance model[35] and should be interpreted physically by smearing the amplitude in x_F or including transverse momentum fluctuations. The physical fragmentation function will thus fall rapidly to zero at the point where the rapid oscillations set in and remain so for all smaller x_F.[36] We will treat this question and the phenomenological implications of this formula at length in a future publication.[15]

(iii) High-energy meson-meson scattering. It is known[10,11] that forward hadron-hadron scattering in QCD_2 has Regge behavior $A \sim s^{-\beta_b - \beta_d}$ arising from the annihilation or exchange of quarks b and d for $s \to \infty$. In the original paper[11] it was shown that the same power is obtained for both $s \to +\infty$ and $s \to -\infty$, but neither the identity of residues required by analyticity nor the correct relationship between real and imaginary parts on the real axis was established. In Ref. 14 we give a formal proof of analyticity for this amplitude. Here we give an explicit illustration: high-energy behavior in the case where one of the mesons m is highly excited[32] and scatters into another excited state m' such that $\mu_m{}^2 - \mu_{m'}{}^2 \ll \mu_m{}^2$. Using the WKB wave functions we are able to obtain a relatively simple and completely explicit form for the Regge residue and hence can now claim

$$A_{st} \simeq \frac{4\pi^2}{N_C} C_n^{ba} C_{n'}^{da} \frac{\sin\pi\beta_b \sin\pi\beta_d}{\sin\pi(\beta_b+\beta_d)} (-s/\mu_m{}^2)^{-\beta_b-\beta_d} \tag{4.15}$$

corresponding to the sum of diagrams in Fig. 14.

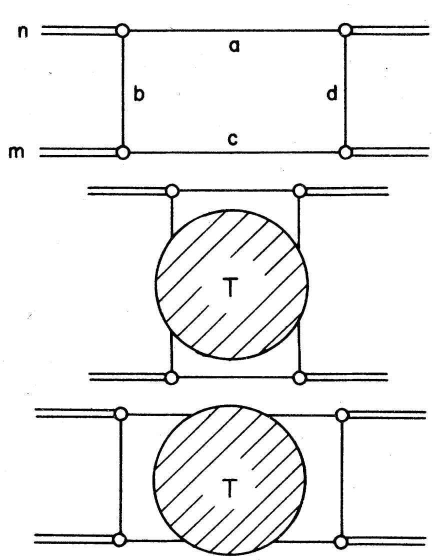

FIG. 14. Covariant Feynman diagrams contributing to Regge behavior in QCD_2. The T matrix is the sum over gluon exchanges given in (2.5) and (2.11).

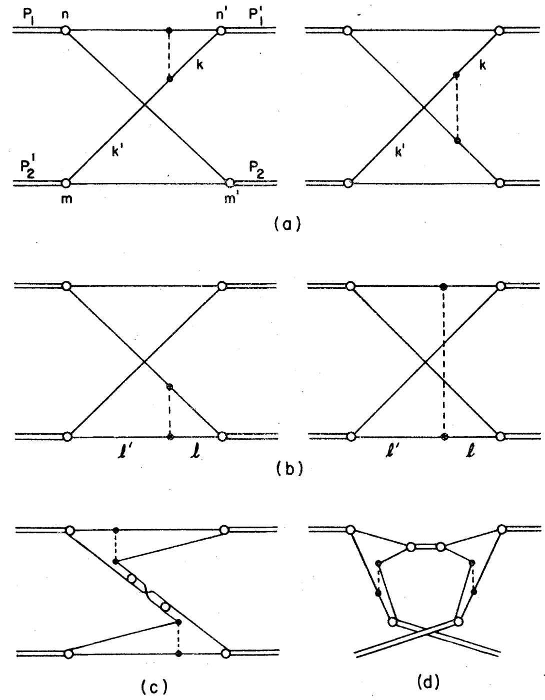

FIG. 15. Infinite-momentum frame diagrams for A_{st} for $s < 0$. (a) t-channel gluon exchange. (b) u-channel gluon exchange. (c) t-channel bound-state exchange. (d) u-channel bound-state exchange. In (c) and (d) only one of four time orderings is shown.

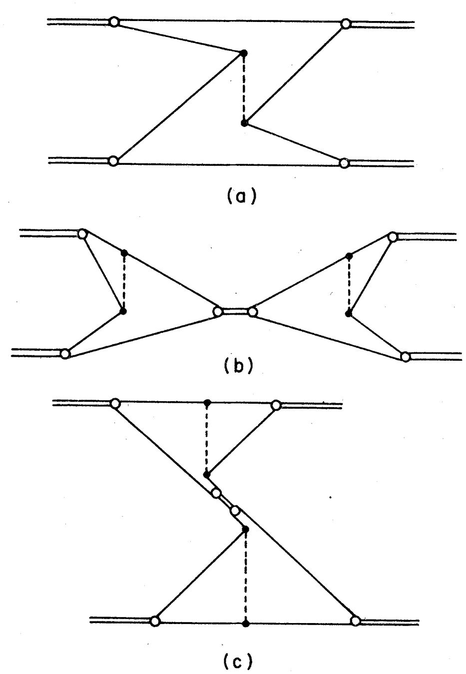

FIG. 16. Diagrams for A_{st} for $s > 0$. (a) t-channel gluon exchange. (b) s-channel poles. (c) t-channel poles. In (b) and (c) only one of four time orderings is shown.

In addition to the phenomena connected with the WKB wave functions illustrated in the preceding calculations, the Regge limit calculations feature a certain amount of tedium, so we relegate their details to Appendix C. In general the wave function $\phi_n^{a\bar{b}} \simeq (1/s)^{\beta_b} C_n^{ba}$ and $\phi_{n'}^{a\bar{d}} \simeq (1/s)^{\beta_d} C_n^{da}$, contributing the Regge power factor. For $s \to -\infty$ only the "gluon" exchange graphs of Fig. 15 contribute. The interior WKB region dominates and the two wave functions $\phi_m^{c\bar{b}}$ and $\phi_m^{c\bar{d}}$ oscillate with the same frequency [even in the graphs of Fig. 16(b) where they occur in separate integrals—this effect is due to the long-distance gluon singularity]. For $s \to +\infty$ the t-channel gluon exchange contribution Fig. 16(a) is very similar to the t-channel gluon graphs for $s \to -\infty$, and the s-channel pole calculation is practically identical to the form-factor computation in subsection (i). The vanishing of the complicated t-channel pole diagrams in both cases Figs. 15(c) and 16(c) (due to the assumption $\mu_m{}^2 - \mu_{m'}{}^2 \ll \mu_m{}^2$) is an essential ingredient in the simplicity of the result (4.15).

V. CONCLUSION

The results of this paper are summarized in the Introduction. We believe that a considerable amount of mathematical control over QCD_2 in the $1/N_C$ expansion has now been achieved. Analyticity is well understood both in a formal sense[14] and in the explicit asymptotic calculations given here. Asymptotic limits can be reliably calculated since the complete solution of the WKB problem is now known. Therefore we regard the light-cone gauge formulation of QCD_2 as providing a fully respectable model quantum field theory of hadrons built out of confined but asymptotically free quarks bound by a vector gluon. It is distinguished at this moment by being the only such model available and thus should serve as an invaluable guide, inspiration, and testing ground for phenomenological ideas about QCD_4, especially when confinement plays a role.

The main remaining technical complication in the model is the lack of manifest parity invariance in the light-cone gauge. As a consequence asymptotic amplitudes derived in one infinite-momentum frame are not obviously equal to those obtained in the parity inverted frame; parity must be assumed and the resultant "parity identity" used in order to get simple-looking formulas. The identity we prove to show asymptotic freedom on the real axis (3.35) also establishes the correct parity relations for scalar and pseudoscalar quark densities taken between the vacuum and an excited meson state.[6,7] The parity identities involved in deriving the Drell-Yan formula for lepton pair production[8] (as well as another identity which may be obtained from inclusive annihilation by repeating the derivation of Sec. IV B for a fragment whose momentum is a fixed fraction of q_+) are linear and homogeneous in 't Hooft's wave function $\phi_n^{a\bar{b}}$ but convolute it with the boundary layer function ϕ^a. Though we have not attempted it, it should now be possible to prove these identities since the boundary layer function is actually known [cf. (3.20) and (3.34)]. This may be worthwhile in light of Wu's[18] criticism of the consistency of the principal-value prescription in the light-cone gauge. Unfortunately the parity identities for factorized Regge residues[10,11] still look difficult, in large part due to the odious t-channel pole graphs.

We have noted above how the confining potential and the resultant end-point singularities in the wave function (which we believe to be a general consequence of confinement[14]) make the derivation of the WKB turning-point conditions unusually difficult. We expect that the techniques developed here to solve this problem may well prove useful when and if a relativistic radial wave equation is derived from QCD_4.

More important for the present, however, is the fact that we have in our hands a concrete model which we believe is qualitatively applicable to physical longitudinal processes. The calculations of Sec. IV show (completely for the first time) that both hard (physical region asymptotic freedom) and soft (dual Regge behavior in hadronic collisions) phenomena emerge consistently from a unified set of asymptotic bound-state properties. Most interesting, moreover, are the results for processes that in general are neither clearly hard (i.e., not light-cone dominated) nor controlled *a priori* by Regge singularities and duality. The asymptotic behavior of form factors and the threshold dependence of structure functions, like Regge behavior, reflect the distribution of slow quarks in the valence component of the hadron's wave function. The quark mass dependent power which characterizes the latter is a new type of singularity that arises directly from the confining potential.[14] In the timelike domain, exclusive- and inclusive-scaling amplitudes for hadron production in annihilation acquire the phases that analyticity dictates must accompany such noninteger powers through intermediate-state rescattering prior to quark fragmentation (as shown in Sec. IV). We have, furthermore, found the same phenomena in inclusive deep-inelastic leptoproduction;[15] the consequences include necessary modifications of naive universality and new interference effects. Details of these calculations and a thorough discussion of the new physics will be given in a forthcoming paper.[15]

ACKNOWLEDGMENTS

R. C. B. wishes to express thanks to the theory groups at CERN and MIT for their hospitality. W. L. S. thanks the theory group at the University of Washington for its hospitality and support during the summer of 1977 while part of this work was being done. J. H. W. wishes to acknowledge the hospitality of the theory groups at SLAC and the University of California at Santa Cruz. We thank Miguel Furman and Terry Schalk for advice on computer programming. We would also like to acknowledge many helpful discussions with R. Anishetty, M. Baker, J. Mandula, M. Nauenberg, C. Thorn, and T. T. Wu. Two of us (R. C. B. and J. H. W.) acknowledge receipt of A. P. Sloan Foundation fellowships. This work was supported in part by the U. S. Department of Energy and the National Science Foundation.

APPENDIX A: BOUNDARY LAYER FUNCTION $\psi(\lambda)$ IN THE $\lambda \to \pm i\infty$ LIMIT

In this appendix we calculate the asymptotic limit for the transformed boundary layer function

$$\psi(\lambda) = \int_0^\infty d\xi\, \xi^{\lambda-1}\phi^a(\xi) \quad \text{(A1)}$$

as $\lambda \to \pm i\infty$. This is determined solely by the WKB approximation for $\phi^a(\xi)$ in the range $\Lambda < \xi < \infty$ where Λ is arbitrarily large:

$$\psi(\lambda_R + i\lambda_I) \simeq \int_0^\Lambda d\xi\, \xi^{\lambda_R - 1 + i\lambda_I}\phi^a(\xi) + \int_\Lambda^\infty d\xi\, \xi^{\lambda_R - 1 + i\lambda_I}\sqrt{2}\sin[\xi/\pi + \delta^a(\xi)]\,. \quad \text{(A2)}$$

As $\lambda_I \to \pm\infty$, the first term is damped by the exponent $\exp(i\lambda_I \ln\xi)$, and is therefore of order $1/\lambda_I$. On the second term, we can use stationary-phase techniques to get the leading term. With the WKB phase

$$\pi\delta_n^a(\xi) = -C(m_a^2) - m_a^2\ln(\xi/\pi^2) + \pi^2/8$$

the second term has the two exponential terms $\mp i(2)^{-1/2}\exp[if_\pm(\xi)]$ where

$$f_\pm(\xi) = [\lambda_I + i(\lambda_R - 1) \mp m_a^2]\ln\xi \pm \xi/\pi \mp (C(m_a^2) - \pi^2/8 - 2m_a^2\ln\pi)\,. \quad \text{(A3)}$$

The stationary points at $(d/d\xi)f_\pm(\xi) = 0$ are

$$\xi_0 = \mp\pi\lambda_I + m_a^2 \pm \pi(\lambda_R - 1)\,, \quad \text{(A4)}$$

and the point at $\xi_0 \simeq +\pi\lambda_I$ gives the dominant contribution to the contour on the positive axis. Hence by the use of stationary-phase techniques

$$\psi(\lambda) \simeq i/\sqrt{2}\, e^{if_-(\xi_0)} \int_{-\infty}^{+\infty} d\xi\, e^{-i(\xi - \pi\lambda_I)^2/2\pi^2\lambda_I} = \frac{i\pi}{\sqrt{2}}(2\pi\lambda_I)^{1/2} e^{-i\pi/4} e^{if_-(\xi_0)}\,. \quad \text{(A5)}$$

Expanding the expression for $f(\xi_0)$ to $O(1/\lambda_I)$ we have the leading term for $\psi(\lambda) = \psi^*(\lambda^*)$ as $\lambda_I \to +\infty$,

$$\psi(\lambda) \simeq \pi(\pi\lambda_I)^{\lambda_R - 1/2}\exp\left\{i\left[\lambda_I\ln(\pi\lambda_I) - \lambda_I + \frac{m_a^2}{\pi}\ln(\lambda_I/\pi) + \frac{C(m_a^2)}{\pi} + \frac{\pi}{8}\right]\right\}. \quad \text{(A6)}$$

This term is the dominant contribution for $\lambda_R > -\frac{1}{2}$. In the explicit solution for this function $\psi(\lambda)$ of Appendix B this formula is verified (up to a constant factor) and the unknown phase $e^{iC/\pi}$ is computed.

APPENDIX B: SOLUTION TO THE BOUNDARY LAYER EQUATION

Here we construct the boundary layer function (3.9) $\phi^a(\xi)$ by solving the difference equation [see Eq. (3.19) with $m_a^2 = -\pi\beta\cot\pi\beta$]

$$\psi(\lambda + 1) = (\pi\lambda\cot\pi\lambda - m_a^2)\psi(\lambda) \quad \text{(B1)}$$

for its Mellin transform

$$\psi(\lambda) = \int_0^\infty d\xi\, \xi^{\lambda-1}\phi^a(\xi)\,. \quad \text{(B2)}$$

To see the difficulty in this problem consider constructing the solution $\psi_0(\lambda)$ for $m_a^2 = 0$. Obviously a *particular* solution, for example, $\psi_0 = \Gamma(\lambda)(\pi\cot\pi\lambda)^\lambda$, can be constructed but that is not likely to be the *right one.* The general solution can have a multiplicative periodic factor $P(\lambda) = P(\lambda + 1)$. The problem is to specify *uniquely* the correct solution and clearly $\Gamma(\lambda)(\pi\cot\pi\lambda)^\lambda$, which has disastrous analytic properties at $\lambda = \frac{1}{2}$, is not likely to be the appropriate one.

To specify uniquely the solution we first notice from the definition (B2) of ψ and the boundary conditions on $\phi^a(\xi)$ in (3.12) and (3.21) that $\psi(\lambda)$ is analytic for $-\beta < \text{Re} < 1$. Moreover, by iterating the difference equation outside this strip ($-\beta < \text{Re}\lambda < 1$), we see that $\psi(\lambda)$ *is a meromorphic function* with poles to the left (at $\lambda = -\beta, -1-\beta_1, -2-\beta_2, \ldots$)

and to the right (at $\lambda=2,3,4,\ldots$) arising from the zeros and poles of $\pi\lambda\cot\pi\lambda-m_a^2$. To avoid unwanted entire factors (such as $\cos 2\pi\lambda$) we need to add an asymptotic condition as $\mathrm{Im}\lambda=\lambda_I\to\pm\infty$. From Appendix A, we have the constraint for $\mathrm{Re}\lambda=\lambda_R>-\frac{1}{2}$ that

$$|\psi(\lambda_R+i\lambda_I)|\underset{\lambda_I\to\infty}{\simeq}\pi(\pi\lambda_I)^{\lambda_R-1/2} \tag{B3}$$

and ψ is real for real λ $[\psi^*(\lambda)=\psi(\lambda^*)]$. This asymptotic condition with analyticity in a strip $-\beta<\lambda_R<2$ determines uniquely the solution to (B1) for $\psi(\lambda)$ as we will now see.

First we construct the solution for $m_a^2=0$ by considering the difference equation

$$\frac{\psi_0'(\lambda+1)}{\psi_0(\lambda+1)}=\frac{1}{\lambda}+\frac{2\pi}{\sin 2\pi\lambda}+\frac{\psi_0'(\lambda)}{\psi_0(\lambda)} \tag{B4}$$

for the logarithmic derivative of $\psi_0(\lambda)$. Now to achieve a meromorphic solution ψ, we must have a logarithmic derivative with simple poles

$$\frac{\psi_0'(\lambda)}{\psi_0(\lambda)}=\frac{d}{d\lambda}\ln\Gamma(\lambda)+\frac{2\pi\lambda}{\sin 2\pi\lambda}+\text{periodic function}. \tag{B5}$$

The additive periodic function is chosen so that $\psi_0(\lambda)$ has no singularities in $-\frac{1}{2}<\mathrm{Re}\lambda<2$. Applying the normalization condition (B3) we find the unique solution

$$\psi_0(\lambda)=\pi^\lambda\Gamma(\lambda)\exp\left(2\pi\int_0^{\lambda-1}du\frac{u+\frac{1}{2}\sin^2\pi\lambda}{\sin 2\pi u}\right). \tag{B6}$$

To find the solution $\psi(\lambda)$ for $m_a^2\neq 0$ we have had to resort to an infinite product. Consider the new factor required for $m_a^2\neq 0$,

$$R(\lambda)=\frac{\psi(\lambda)}{\psi_0(\lambda)}. \tag{B7}$$

Since the normalization condition (B3) is independent of m_a^2 we need only require $|R(\lambda)|\simeq 1$ as $\lambda_I\to\infty$. This ratio $R(\lambda)$ is also meromorphic and satisfies the difference equation

$$R(\lambda+1)=\left(1+\frac{m_a^2}{\pi\lambda\cot\pi\lambda}\right)R(\lambda). \tag{B8}$$

We consider the solution

$$R(\lambda)=\frac{\Gamma(\lambda+(m_a^2/\pi)\tan\pi\lambda)}{\Gamma(\lambda)}P(\lambda), \tag{B9}$$

where $P(\lambda)$ is an unspecified periodic function. Our particular solution has an accumulation point of poles at $\lambda=\frac{1}{2}$ from the roots $\lambda=\beta_n$ ($\beta_0=\beta$) of

$$\beta_n+n+\frac{m_a^2}{\pi}\tan\pi\beta_n=0 \tag{B10}$$

in the interval $0<\beta_n<1$. The factor $P(\lambda)$ must be chosen to cancel these poles. By the standard product expansion, the polynomial in $z=(m^2/\pi)\tan\pi\lambda$ with zeros at $z=-\beta_n-n$ for $n=0,1,2,\ldots$ is given by

$$P(z)=P(0)e^{\tilde\gamma z}\prod_{n=0}^{\infty}\left(1+\frac{z}{\beta_n+n}\right)e^{-z/(\beta_n+n)}. \tag{B11}$$

Aside from the arbitrary constants $P(0)$ and $\tilde\gamma$, $P(z)$ is the unique periodic function with the desired roots. The constant $\tilde\gamma$ is fixed by the requirement that $R(\lambda)$ be analytic as $\lambda\to\frac{1}{2}$. By demanding uniform convergence[37] for the entire product for $R(\lambda)$ (including expanding out the Γ functions as well) on a closed curve circling $\lambda=\frac{1}{2}$, we see that analyticity at $\lambda=\frac{1}{2}$ requires

$$\tilde\gamma=\gamma+\frac{1}{\beta_0}+\sum_{n=1}^{\infty}\left(\frac{1}{\beta_n+n}-\frac{1}{n}\right), \tag{B12}$$

where γ is Euler's constant. This gives the product expression for $\psi(\lambda)\equiv\psi_0(\lambda)R(\lambda)$ as

$$\psi(\lambda)=P(0)\psi_0(\lambda)\prod_{n=0}^{\infty}\frac{1+(m_a^2/\pi)(\tan\pi\lambda)/(\beta_n+n)}{1+(m_a^2/\pi)(\tan\pi\lambda)/(\lambda+n)}. \tag{B13}$$

To fix the normalization, we must compute the limit of $|R(\lambda_R+i\lambda_I)|^2$ as $\lambda_I\to\infty$. This leads immediately to $|R|^2=P^2(0)e^{-m_a^2}\Pi(m_a^2)$, where

$$\Pi(m_a^2)=\prod_{n=0}^{\infty}\left(1+\frac{m_a^2}{\pi}\frac{1}{(\beta_n+n)^2}\right). \tag{B14}$$

We can evaluate the product by taking the logarithmic derivative with respect to m_a^2,

$$\frac{\Pi'(m_a^2)}{\Pi(m_a^2)}=2\sum_{n=0}^{\infty}\frac{m_a^2}{m_a^2(1+m_a^2)+\pi^2(\beta_n+n)^2}, \tag{B15}$$

and doing the sum by converting it into an integral over z,

$$\frac{\Pi'(m_a^2)}{\Pi(m_a^2)}=\oint\frac{dz}{2\pi i}\frac{Q'(z)}{Q(z)}\left(\frac{m_a^2}{m_a^2(1+m_a^2)+\pi^2z^2}\right)-\frac{1}{1+m_a^2}, \tag{B16}$$

where $Q=\pi z\cos\pi z+m_a^2\sin\pi z$ has roots at $z=0$ and $\pm(\beta_n+n)$, $n=0,1,2,\ldots$. Expanding the contour (see Fig. 17) the poles at $\pi z=\pm i[m_a^2(1+m_a^2)]^{1/2}$ are picked up using Cauchy's theorem to get

$$\frac{\Pi'(m_a^2)}{\Pi(m_a^2)}=1-\frac{1}{1+m_a^2},$$

or

$$|R|^2=P^2(0)e^{-m_a^2}\left(\frac{e^{m_a^2}}{1+m_a^2}\right)=1 \tag{B17}$$

and $P(0)=(1+m_a)^{1/2}$. The normalization condition gives the important identity (see Sec. IV A)

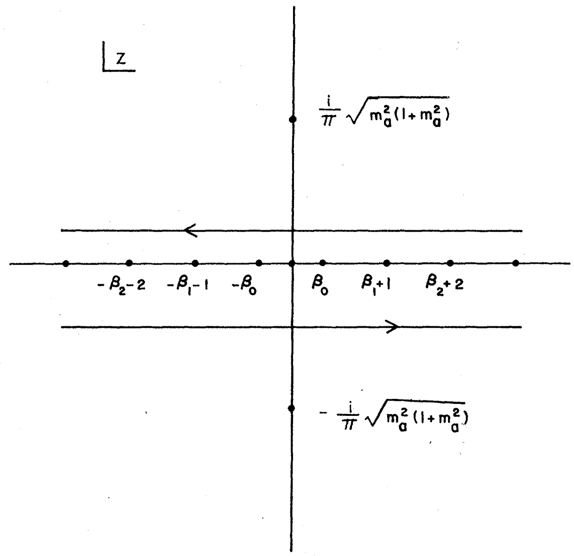

FIG. 17. Contour in (B16) for doing the sum in (B15).

$$\psi(0)=\int_0^\infty d\xi\,\xi^{-1}\phi^a(\xi)=\frac{\pi}{(1+m_a^2)^{1/2}}. \tag{B18}$$

Finally to calculate the WKB constant $C(m_a^2)$ we need to compute the phase of $\psi(\lambda)$ as $\lambda_I\to\infty$. Combining Eqs. (B9), (B11), and (B12), it is straightforward to express the phase of $R(\lambda)$ for $\lambda_I\to\infty$ as the sum

$$\arg R(\lambda)\simeq\frac{m_a^2}{\pi}(\ln\lambda_I+\gamma)+\pi(\beta_0-\tfrac{1}{2})+\sum_{n=1}^{\infty}\left[\pi(\beta_n-\tfrac{1}{2})-\frac{m_a^2}{\pi n}\right]. \tag{B19}$$

Now comparing (B19) with the phase for $\psi(\lambda)/\psi_0(\lambda)$ from the WKB form [Appendix A, Eq. (A6)], we find a series expansion for $C(m_a^2)$,

$$C(m_a^2)=\frac{m_a^2}{\pi}(\gamma+\ln\pi)+\pi(\beta_0-\tfrac{1}{2})+\sum_{n=1}^{\infty}\left[\pi(\beta_n-\tfrac{1}{2})-\frac{m_a^2}{\pi n}\right]. \tag{B20}$$

To establish the equivalence of this sum to our integral expression (3.32) for $C(m_a^2)$ one rewrites the integral to run from $y=-\infty$ to $+\infty$ in a complex $z=x+iy$ plane and then pushes the contour to the right ($x\to\infty$) picking up each of the poles. Special care needs to be taken with the second term in the integrand which has a surface term at $x=\infty$,

$$\lim_{x\to\infty}\int_{x-i\infty}^{x+i\infty}\frac{dz}{2i}\frac{m_a^2}{z\tan z+m_a^2}\frac{2z}{\sin 2z}=m_a^2. \tag{B21}$$

The Euler constant γ comes from the last term in the integral (3.32) using its definition

$$\gamma=\lim_{N\to\infty}\left(\sum_{n=1}^{N}\frac{1}{n}-\ln N\right). \tag{B22}$$

Hence the more elegant but indirect approach in the text for computing $C(m_a^2)$ is confirmed by the direct construction of the solution (B13) to the boundary layer equation (3.10) for 't Hooft's integral equation.

APPENDIX C: HIGH-ENERGY MESON-MESON SCATTERING

We consider the process $n+m\to n'+m'$ in the limit

$$|s|\gg\mu_m^2,\mu_{m'}^2\gg\mu_m^2-\mu_{m'}^2,\mu_n^2,\mu_{n'}^2. \tag{C1}$$

We study the amplitude A_{st} which has bound-state poles in the $s(a\bar{c})$ and $t(d\bar{b})$ channels. In general this amplitude has the contributions shown in Fig. 14.

First consider $s\to-\infty$. Evaluating the + component momentum integrals yields the x_- ordered graphs in Fig. 15 (see Sec. II.2 of Ref. 11). The t-channel gluon exchange graphs [Fig. 15(a)] are

$$A_{st}^{(a)}=\frac{4\pi}{N_C}\mathrm{P}\int_0^{p'_{2-}}dk'_-\int_0^{p'_{1-}}\frac{dk_-}{(k_--k'_-)^2}\left[\phi_n^{b\bar{a}}\left(\frac{p_{2-}-p'_{2-}+k'_-}{p_{1-}}\right)-\phi_n^{b\bar{a}}\left(\frac{p_{2-}-p'_{2-}+k_-}{p_{1-}}\right)\right]\phi_{n'}^{d\bar{a}}\left(\frac{k_-}{p'_{1-}}\right)\phi_{m'}^{d\bar{c}}\left(\frac{k'_-}{p'_{2-}}\right)\phi_m^{c\bar{b}}\left(\frac{p_{2-}-p'_{2-}+k'_-}{p_{2-}}\right), \tag{C2}$$

the dominant behavior for $s\to-\infty$ arises from finite η where $k_-=\eta p'_{2-}$. Writing also $k'_-=xp'_{2-}$ we have

$$A_{st}^{(a)}\simeq(-s/\mu_m^2)^{-\beta_b-\beta_d}(4\pi/N_C)C_n^{ba}C_{n'}^{da}\mathrm{P}\int_0^1 dx\int_0^\infty d\eta\frac{x^{\beta_b}-\eta^{\beta_b}}{(x-\eta)^2}\eta^{\beta_d}\phi_{m'}^{c\bar{d}}(1-x)\phi_m^{c\bar{b}}\left(\frac{\mu_{m'}^2}{\mu_m^2}(1-x)\right). \tag{C3}$$

Using the WKB wave functions gives

$$\phi_{m'}^{c\bar{d}}(1-x)\phi_m^{c\bar{b}}\left(\frac{\mu_{m'}^2}{\mu_m^2}(1-x)\right)\simeq\cos\frac{1}{\pi}[(m_d^2-m_b^2)\ln x]\,.$$

The integrals can then be evaluated and we find

$$A_{st}^{(a)}\simeq(-s/\mu_m^2)(4\pi/N_C)C_n^{ba}C_{n'}^{da}\frac{\sin\pi\beta_b\sin\pi\beta_d}{\sin\pi(\beta_b+\beta_d)}\times\left\{\frac{(\beta_b+\beta_d)[\beta_d\sin^2\pi\beta_b-\beta_b\sin\beta_b\sin\pi\beta_d\cos\pi(\beta_b+\beta_d)]}{\beta_b^2\sin^2\pi\beta_d+\beta_\alpha^2\sin^2\pi\beta_b-2\beta_b\beta_d\sin\pi\beta_b\sin\pi\beta_d\cos\pi(\beta_b+\beta_d)}\right\}. \tag{C4}$$

The u-channel gluon exchange graphs of Fig. 15(b) are

$$A_{st}^{(b)}=\frac{4\pi}{N_C}\,\mathrm{P}\int_0^{p_{2-}}dl_-\int_0^{p'_{2-}}dl'_-\frac{\phi_n^{b\bar{a}}\left(\frac{p_{2-}-l'_-}{p_{1-}}\right)-\phi_n^{b\bar{a}}\left(\frac{p_{2-}-l_-}{p_{1-}}\right)}{(l_--l'_-)^2}\,\phi_{n'}^{d\bar{a}}\left(\frac{p_{2-}-l'_-}{p'_{1-}}\right)\phi_{m'}^{c\bar{d}}\left(\frac{l'_-}{p'_{2-}}\right)\phi_m^{c\bar{b}}\left(\frac{l_-}{p_{2-}}\right). \tag{C5}$$

Writing $l_-=xp_{2-}$ and $l'_-=yp_{2-}$ and taking $s\to-\infty$ gives

$$A_{st}^{(b)}\simeq(-s/\mu_m^2)^{-\beta_b-\beta_d}\frac{4\pi}{N_C}C_n^{ba}C_{n'}^{da}\int_0^1dx\int_0^1dy\frac{[(1-y)^{\beta_b}-(1-x)^{\beta_b}]}{(x-y)^2}(1-y)^{\beta_d}\phi_m^{c\bar{b}}(x)\phi_{m'}^{c\bar{d}}\left(\frac{\mu_m^2}{\mu_{m'}^2}y\right). \tag{C6}$$

The range of integration $x\approx y$ dominates. Using the WKB wave function for $\phi_m^{c\bar{b}}$, closing the x integration contour in the appropriate half planes, and picking up the principal-value poles gives

$$\int_0^1dx\,\phi_m^{c\bar{b}}(x)\frac{(1-x)^{\beta_b}-(1-y)^{\beta_b}}{(x-y)^2}\simeq\sqrt{2}\pi\beta_b(1-y)^{\beta_b-1}\cos\frac{1}{\pi}[\mu_m^2y-m_c^2\ln(y\mu_m^2/\pi^2)+m_b^2\ln(1-y)]\,.$$

The y integral in (C6) can then be evaluated with the result

$$A_{st}^{(b)}\simeq(-s/\mu_m^2)(4\pi/N_C)C_n^{ba}C_{n'}^{da}\sin\pi\beta_b\sin\pi\beta_d\left\{\frac{\beta_b[\beta_b\cos\pi\beta_b\sin\pi\beta_d-\beta_d\sin\pi\beta_b\cos\pi\beta_d]}{\beta_b^2\sin^2\pi\beta_d+\beta_d^2\sin^2\pi\beta_b-2\beta_b\beta_d\sin\pi\beta_b\sin\pi\beta_d\cos\pi(\beta_b+\beta_d)}\right\}. \tag{C7}$$

The t-channel bound-state pole terms of Fig. 15(c) vanish due to vanishing range of integration as $t\sim0$. The u-channel pole terms of Fig. 15(d) are also negligible in the asymptotic limit. From Eqs. (C14) and (C7) we thus obtain

$$A_{st}\simeq\frac{4\pi^2}{N_C}C_n^{ba}C_{n'}^{da}\frac{\sin\pi\beta_b\sin\pi\beta_d}{\sin\pi(\beta_b+\beta_d)}\left(\frac{-s}{\mu_m^2}\right)^{-\beta_b-\beta_d} \tag{C8}$$

for $s\to-\infty$.

We now consider $s\to+\infty\pm i\epsilon$. The time-ordered perturbation-theory diagrams in this case are shown in Fig. 16 (see Sec. I.3 of Ref. 11). The t-channel gluon exchange graph of Fig. 16(a) is

$$A_{st}^{(a)}=-\frac{4\pi}{N_C}\int_0^{p'_{1-}}dk_-\int_0^{p_{2-}}dl_-\frac{1}{(k_-+p'_{2-}-l_-)^2}\,\phi_n^{b\bar{a}}\left(\frac{p'_{2-}-p_{2-}+k_-}{p_{1-}}\right)\phi_{n'}^{d\bar{a}}\left(\frac{k_-}{p_{1-}}\right)\phi_m^{c\bar{b}}\left(\frac{l_-}{p_{2-}}\right)\phi_{m'}^{c\bar{d}}\left(\frac{l_-}{p'_{2-}}\right). \tag{C9}$$

Writing $k_-=\eta p'_{2-}$ and $l_-=xp_{2-}$ and observing that the dominant behavior comes from η finite gives

$$A_{st}^{(a)}\simeq-\frac{4\pi}{N_C}C_n^{ba}C_{n'}^{da}(s/\mu_m^2)^{-\beta_b-\beta_d}\int_0^\infty d\eta\int_0^1dx\,\eta^{\beta_b+\beta_d}\,\frac{\phi_m^{c\bar{b}}(x)\phi_{m'}^{c\bar{d}}\left(\frac{\mu_m^2}{\mu_{m'}^2}x\right)}{[\eta+(1-x)]^2}\,. \tag{C10}$$

The integrals can be evaluated when the WKB wave functions are inserted and we have

$$A_{st}^{(a)}\simeq-\frac{4\pi}{N_C}C_n^{ba}C_{n'}^{da}(s/\mu_m^2)^{-\beta_b-\beta_d}\frac{\sin\pi\beta_b\sin\pi\beta_d}{\sin\pi(\beta_b+\beta_d)}\left[\frac{(\beta_b+\beta_d)^2\sin\pi\beta_b\sin\pi\beta_d}{\beta_b^2\sin^2\pi\beta_d+\beta_d^2\sin\pi\beta_b-2\beta_b\beta_d\sin\pi\beta_b\sin\pi\beta_d\cos\pi(\beta_b+\beta_d)}\right]. \tag{C11}$$

The s-channel pole terms have the form[11]

$$A_{st}^{(b)} \simeq -\frac{4\pi}{N_C} C_n^{ba} C_{n'}^{da} (s/\mu_m^2)^{-\beta_b-\beta_d} \frac{1}{\pi^2}$$
$$\times \int_0^\infty d\lambda (1-\lambda \pm i\epsilon)^{-1} \left[\int_0^\infty d\eta \int_0^1 dx \frac{\eta^{\beta_b}}{(\eta+x)^2} \phi_m^{c\bar{b}}(1-x) \phi_l^{c\bar{a}}\left(\frac{s}{\mu_m^2}\lambda(1-x)\right)\right]$$
$$\times \left[\int_0^\infty d\eta \int_0^1 dx \frac{\eta^{\beta_d}}{(\eta+x)^2} \phi_{m'}^{c\bar{d}}(1-x) \phi_l^{c\bar{a}}\left(\frac{s}{\mu_{m'}^2}\lambda(1-x)\right)\right], \tag{C12}$$

where $\mu_l^2 \equiv \lambda s$. Inserting the WKB forms for the remaining wave functions and evaluating the η and η' integrals gives

$$A_{st}^{(b)} \simeq -\frac{4\pi}{N_C} C_n^{ba} C_{n'}^{da} \frac{\beta_b}{\sin\pi\beta_b} \frac{\beta_d}{\sin\pi\beta_\alpha} (s/\mu_m^2)^{-\beta_b-\beta_d}$$
$$\times \int_0^\infty d\lambda (1-\lambda \pm i\epsilon)^{-1} \left\{ \int_0^1 dx\, x^{\beta_b-1} \cos\frac{1}{\pi}[\mu_m^2(1-x)(1-\lambda)+m_b^2 \ln x] \right\}$$
$$\times \left\{ \int_0^1 dx\, x^{\beta_d-1} \cos\frac{1}{\pi}[\mu_{m'}^2(1-x)(1-\lambda)+m_d^2 \ln x] \right\}. \tag{C13}$$

The cosines can be expressed in terms of exponentials and the λ integral evaluated by then closing in the appropriate half plane to obtain

$$A_{st}^{(b)} \simeq -\frac{4\pi}{N_C} C_n^{ba} C_{n'}^{da} \frac{\beta_b \beta_d}{\sin\pi\beta_b \sin\pi\beta_d} (s/\mu_m^2)^{-\beta_b-\beta_d}$$
$$\times \left(\frac{\mp i\pi}{2}\right) \int_0^1 dx \int_0^1 dx'\, x^{\beta_b-1} x'^{\beta_d-1} [x^{\mp i m_b^2/\pi} x'^{\mp i m_d^2/\pi}$$
$$+ \theta(x-x') e^{\pm i m_b^2/\pi} e^{\mp i m_d^2/\pi} + \theta(x'-x) e^{\mp i m_b^2/\pi} e^{\pm i m_a^2/\pi}]. \tag{C14}$$

The remaining integrals can now be easily evaluated.

The t-channel pole terms in Fig. 16(c) again vanish as $t \sim 0$. Equations (C11) and (C14) give (after a considerable amount of algebra)

$$A_{st} \simeq \frac{4\pi^2}{N_C} C_n^{ba} C_{n'}^{da} \frac{\sin\pi\beta_b \sin\pi\beta_d}{\sin\pi(\beta_b+\beta_d)} e^{\pm i\pi(\beta_b+\beta_d)} (s/\mu_m^2)^{-\beta_b-\beta_d} \tag{C15}$$

for $s \to \infty \pm i\epsilon$ as expected on the basis of (C8) and analyticity. This special case of the high-energy limit is thus consistent with analyticity in s.

---

*Deceased.

[1]Summarized by G. Veneziano, Phys. Rep. 9C, 199 (1974), and C. Rebbi, *ibid.* 12C, 1 (1974).

[2]H. Politzer, Phys. Rep. 14C, 129 (1974); more recent developments are reviewed by S. Brodsky, International Symposium on Multiparticle Dynamics, Kayserberg, 1977 (unpublished).

[3]K. Wilson, Phys. Rev. D 10, 2445 (1974); J. Kogut and L. Susskind, *ibid.* 11, 395 (1975); S. Mandelstam, Berkeley report, 1978 (unpublished); C. Callan, R. Dashen, and D. Gross, Phys. Lett. 66B, 375 (1977).

[4]G. 't Hooft, Nucl. Phys. B72, 461 (1974); B75, 461 (1975); *New Phenomena in Subnuclear Physics*, proceedings of the 14th Course of the International School of Subnuclear Physics, Erice, 1975, edited by A. Zichichi (Plenum, New York, 1977). For a review of the formulation and early applications of QCD_2, see J. Ellis, Lectures at Cracow School of Theoretical Physics, Zakopane, Poland, 1977 (unpublished).

[5]P. Federbush and A. Tromba, Phys. Rev. D 15, 2913 (1977).

[6]C. Callan, N. Coote, and D. Gross, Phys. Rev. D 13, 1649 (1976).

[7]M. Einhorn, Phys. Rev. D 14, 3451 (1976).

[8]J. Kripfganz and M. Schmidt, Nucl. Phys. B125, 323 (1977). This derivation of the Drell-Yan formula assumes two identities in QCD_2—one is true if parity is preserved in the $A_- = 0$ gauge while the other is the same normalization condition needed for agreement with asymptotic freedom in the annihilation and deep-inelastic total cross sections.

[9]M. Einhorn, Phys. Rev. D 15, 3037 (1977).

[10]M. Einhorn, S. Nussinov, and E. Rabinovici, Phys. Rev. D 15, 2282 (1977).

[11]R. Brower, J. Ellis, M. Schmidt, and J. Weis, Nucl. Phys. B128, 131 (1977).

[12]R. Brower, J. Ellis, M. Schmidt, and J. Weis, Nucl. Phys. B128, 175 (1977).

[13]M. Einhorn and E. Rabinovici, Nucl. Phys. B128, 421 (1977).

[14]R. Brower, W. Spence, and J. Weis, Phys. Rev. D 18, 499 (1978). Confinement singularities have physical consequences when wave functions are measured as discussed in R. Brower, W. Spence, and J. Weis,

Phys. Rev. Lett. 40, 647 (1978).

[15]R. Anishetty, R. Brower, W. Spence, and J. Weis (unpublished).

[16]It is interesting that the linear potential in one space dimension is the only possible *local* potential. This is because the force is independent of separation $F = -(\partial/\partial x)V(x) = \pm$ const for $V(x) \propto |x|$. Hence we are studying the only covariant and causal field theory expressible in terms of quarks in a static potential.

[17]See Ref. 6 where it is introduced. This regulator only treats the new "confinement" infrared divergence. The familiar infrared mass shell singularities remain in perturbation theory; see the first paper of Ref. 14.

[18]T. T. Wu, Phys. Lett. 71B, 142 (1977).

[19]J. H. Weis, Lectures at the XVIII Cracow School of Theoretical Physics, 1978 (unpublished).

[20]I. Bars, Phys. Rev. Lett. 36, 1521 (1976); Nucl. Phys. B111, 413 (1976).

[21]We will use m_a to also denote the *dimensionless* quark mass. Note that our m_a is $\tilde{m}_a$ in Ref. 11, 12, and 14.

[22]S. Hildebrandt and V. Višnjić, Phys. Rev. D 17, 1618 (1978); Arkiv. Mat. (to be published); S. Hildebrandt, Manuscripta Mathematica 24, 45 (1978).

[23]This formula is easily obtained by expanding the 't Hooft equation near the would-be threshold $x \simeq (m_a + k)/(m_a + m_b)$ in which case it can be approximated by the nonrelativistic Schrödinger equation. A similar result is found in Ref. 6 by a variational method.

[24]A. Hanson, R. Peccei, and M. Prasad, Nucl. Phys. B121, 477 (1977).

[25]S.-S. Shei and H.-S. Tsao, Institute for Advanced Study report, 1977 (unpublished), also construct this explicit matrix form of the 't Hooft equation, but do no numerical calculations. See also Don Tripp, UCSC senior physics thesis, 1977 (unpublished).

[26]S. Weinberg, in Festschrift for I. I. Rabi, Trans. New York Acad. Sci., Vol. 38, 1977.

[27]In Ref. 25 the same formulation of the WKB problem developed in this section is applied to QCD_2 for scalar quarks. Since these authors do not recognize the failure of the classical WKB turning point conditions their phase shifts are missing important terms and the constant C implied by their quantization condition is incorrect.

[28]This boundary layer (fixed ξ) function is the "scaling" function introduced by Einhorn in Ref. 7.

[29]We are grateful to T. T. Wu for suggested this approach (private communication).

[30]R. Dashen, B. Hasslacher, and A. Neveu, Phys. Rev. D 10, 4114 (1974).

[31]The amplitude has been multiplied by the square root of the sum over intermediate bound states $[\int dl\, \pi\delta(\pi^2 l - s)]^{1/2} = 1/\sqrt{\pi}$. We also explicitly compute only the $-$component to get the invariant amplitude defined by $\langle l|J_\pm(q)|n\rangle = (p_\pm/p\cdot q - q_\pm)F(q^2) \simeq \mp q_\pm F$ for $|q^2| \to \infty$. We follow the formalism of Refs. 7 and 11. Only the contribution in which quark a is struck is explicitly shown.

[32]That great simplifications occur in such massive limits was noted and exploited in Ref. 11. It is only when this happens that we can give detailed answers.

[33]The physics of this case is the subject of the second paper in Ref. 14.

[34]Even in the next order of $1/N_C$, the cancellation of the Pomeron singularity noted in Refs. 12 and 13 is expected to remove the plateau associated with the sea quark distribution, as verified for electroproduction ($x_B \to 0$) by H. Dorn, D. Ebert, and V. Pervushin, Dubna report, 1978 (unpublished).

[35]C. DeTar, K. Kang, C.-I. Tan, and J. H. Weis, Phys. Rev. D 4, 425 (1971), in particular the end of Sec. IV.

[36]V. Višnjić-Triantafillou, Phys. Lett. 76B, 310 (1978), attempts to compute fragmentation functions with the omission of the exponential factor in (4.13). We disagree with his claim that the latter is unimportant for light quarks. This is especially evident for small x_F—see the discussion in the text. We will present our complete numerical calculations of Φ in Ref. 15.

[37]E. C. Titchmarsh, *The Theory of Functions*, 2nd edition (Oxford Univ. Press, London, England, 1939).